

1 **SNORD90 induces glutamatergic signaling following treatment with** 2 **monoaminergic antidepressants**

4 **AUTHORS**

5 Rixing Lin^{1,2,†}, Aron Kos^{3,4,5,†}, Juan Pablo Lopez^{3,4,5}, Julien Dine^{3,4,5}, Laura M. Fiori¹, Jennie
6 Yang¹, Yair Ben-Efraim^{3,4,5}, Zahia Aouabed¹, Pascal Ibrahim^{1,2}, Haruka Mitsuhashi^{1,2}, Tak Pan
7 Wong^{6,7}, El Cherif Ibrahim⁸, Catherine Belzung⁹, Pierre Blier¹⁰, Faranak Farzan¹¹, Benicio N.
8 Frey^{12,13}, Raymond W. Lam¹⁴, Roumen Milev¹⁵, Daniel J. Müller^{16,17}, Sagar V. Parikh¹⁸, Claudio
9 Soares¹⁵, Rudolf Uher^{19,20}, Corina Nagy¹, Naguib Mechawar¹, Jane A. Foster^{12,13,16}, Sidney H.
10 Kennedy^{16,21}, Alon Chen^{3,4,5*}, and Gustavo Turecki^{1*}

12 **AFFILIATIONS**

13 ¹McGill Group for Suicide Studies, Douglas Mental Health University Institute, Department of
14 Psychiatry, McGill University; Montreal, QC, Canada

15 ²Integrated Program in Neuroscience, McGill University; Montreal, QC, Canada

16 ³Department of Stress Neurobiology and Neurogenetics, Max Planck Institute of Psychiatry;
17 Munich, Germany

18 ⁴Department of Brain Sciences, Weizmann Institute of Science; Rehovot, Israel

19 ⁵Department of Molecular Neuroscience, Weizmann Institute of Science; Rehovot, Israel

20 ⁶Neuroscience Division, Douglas Research Centre; Montreal, QC, Canada.

21 ⁷Department of Psychiatry, McGill University; Montreal, QC, Canada.

22 ⁸Aix-Marseille Université, CNRS, INT, Institute Neuroscience Timone; Marseille, France

23 ⁹UMR 1253, iBrain, UFR Sciences et Techniques; Parc Grandmont, Tours, France

24 ¹⁰Mood Disorders Research Unit, University of Ottawa Institute of Mental Health Research;
25 Ottawa, Ontario, Canada.

26 ¹¹eBrain Lab, Simon Fraser University; Surrey, British Columbia, Canada

27 ¹²Department of Psychiatry and Behavioural Neurosciences, McMaster University; Hamilton,
28 ON, Canada

29 ¹³Mood Disorders Program, St. Joseph's Healthcare Hamilton; Hamilton, ON, Canada

30 ¹⁴Department of Psychiatry, University of British Columbia; Vancouver, British Columbia,
31 Canada

32 ¹⁵Departments of Psychiatry and Psychology, Queens University, Providence Care; Kingston,
33 Ontario, Canada

34 ¹⁶Department of Psychiatry, University Health Network, Krembil Research Institute, University
35 of Toronto; Toronto, Ontario, Canada

36 ¹⁷Centre for Addiction and Mental Health; Toronto, Ontario, Canada

37 ¹⁸Department of Psychiatry, University of Michigan; Ann Arbor, Michigan, USA

38 ¹⁹Nova Scotia Health Authority; Halifax, NS, Canada

39 ²⁰Department of Psychiatry, Dalhousie University; Halifax, Nova Scotia, Canada

40 ²¹St Michael's Hospital, Li Ka Shing Knowledge Institute, Centre for Depression and Suicide
41 Studies; Toronto, Ontario, Canada

43 [†]These authors contributed equally to this work

45 *Corresponding author. Email: gustavo.turecki@mcgill.ca

46

47 **ABSTRACT**

48 Most available antidepressants target the serotonergic system, selectively or non-selectively, and
49 yield slow and inconsistent clinical responses, whereas the monoamine changes they elicit do not
50 correlate with treatment response. Recent findings point to the glutamatergic system as a target
51 for rapid acting antidepressants. Investigating different cohorts of depressed individuals treated
52 with serotonergic and other monoaminergic antidepressants, we found that the expression of a
53 small nucleolar RNA, SNORD90, was elevated following treatment response. When we
54 increased SNORD90 levels in the mouse anterior cingulate cortex (ACC), a brain region
55 regulating mood responses, we observed antidepressive-like behaviors. We identified neuregulin
56 3 (NRG3) as one of the targets of SNORD90, which we show is regulated through the
57 accumulation of N6-methyladenosine modifications leading to YTHDF2 mediated RNA decay.
58 We further demonstrate that a decrease in NRG3 expression resulted in increased glutamatergic
59 release in the mouse ACC. These findings support a molecular link between monoaminergic
60 antidepressant treatment and glutamatergic neurotransmission.

61

62 **INTRODUCTION:**

63 Antidepressants are the first line treatment for major depressive disorder (MDD), collectively
64 accounting for one of the most prescribed medications (1). However, response to antidepressant
65 treatment is variable with less than 50% of patients responding to first trial, and up to 40% with
66 no clinical response after two or more trials (2). While most currently available antidepressants
67 act by selectively or non-selectively targeting serotonergic receptors the exact mechanisms by
68 which they effect mood changes and improvements in depression remain unknown. Importantly,
69 although the enhancement of monoamine function, in particular serotonin, can be observed
70 within hours after antidepressant drug administration, clinical improvements are not observed
71 until days or weeks following antidepressant treatment initiation (3-5). The delayed clinical
72 response led researchers to study underlying neurobiological adaptations to understand
73 mechanisms of antidepressant response. Monoamines have been a focus of depression studies
74 since most treatment options target this system. However, given the delayed clinical response
75 other neurotransmitter systems have been gaining interest in depression and particularly the
76 glutamatergic system, which is believed to be the target of rapid acting antidepressants (6, 7).
77 Moreover, recent evidence suggest that monoaminergic antidepressants may act by modulating
78 the glutamatergic system, although it is still unclear through what molecular mechanisms (8, 9).

79
80 In this study, we identified a molecular mechanism whereby monoaminergic antidepressants
81 produce an effect on glutamatergic neurotransmission. We found elevated levels of a small
82 nucleolar RNA (snoRNA), SNORD90, in response to antidepressant drug exposure and report
83 that SNORD90 guides N6-methyladenosine (m6A) modifications onto neuregulin 3 (NRG3),

84 which in turn lead to YTHDF2-mediated down-regulation of NRG3 expression and subsequent
85 increases in glutamatergic release.

86

87 **RESULTS:**

88 **SNORD90 levels are increased in response to monoaminergic antidepressants**

89 We initially examined snoRNA expression using small RNA-sequencing data from peripheral
90 blood samples collected from three independent antidepressant clinical trials (discovery cohort,
91 replication cohort 1 and replication cohort 2) administering duloxetine, escitalopram, or
92 desvenlafaxine. To identify snoRNAs associated with treatment response, we focused our
93 attention on snoRNAs that were differentially expressed between baseline (T0) and eight weeks
94 after treatment (T8), when clinical outcome was ascertained. In doing so, we identified nine
95 snoRNAs in our placebo controlled double blind discovery cohort that had a significant
96 interaction ($p < 0.05$) between time (T0/T8) and treatment outcome (response/non-response)
97 (figure 1A & supplemental table 1-3). In particular, SNORD90 was the only snoRNA that was
98 consistently up-regulated after antidepressant treatment in subjects who responded to treatment
99 across all three independent cohorts (figure 1B & supplemental figure 1). As such, we further
100 investigated SNORD90.

101

102 To better understand if SNORD90 expression has similar changes in the brain following
103 antidepressant treatment as observed in peripheral tissue, we investigated human post-mortem
104 anterior cingulate cortex (ACC), a brain region that plays an important role in the regulation of
105 mood (10, 11). We studied individuals who died while affected with MDD and were or were not
106 treated with antidepressants. We observed a specific up-regulation of SNORD90 in individuals

107 who were depressed when they died and were actively treated with antidepressants (figure 1C).
108 To follow up these results, we investigated the expression of Snord90 in an unpredicted chronic
109 mild stress (UCMS) mouse model, which is commonly used to study depressive-like behaviors
110 in mice. Mice were subjected to UCMS, followed by administration of fluoxetine (12). We
111 specifically profiled the mouse cingulate area 1/2 (cg1/2), a region that is equivalent to the
112 human ACC. Similar to the results observed in humans, we observed a specific up-regulation of
113 Snord90 in the ACC of mice that underwent the UCMS paradigm followed by antidepressant
114 administration, whereas UCMS or antidepressant administration alone did not alter the
115 expression of Snord90 (figure 1D). To assess if the effects observed on the expression of
116 SNORD90 were specific to antidepressants or common to other drugs, we treated human
117 neuronal cells derived from iPSCs and differentiated to a monoaminergic phenotype with several
118 psychotropic drugs, including duloxetine, escitalopram, haloperidol, lithium, or non-
119 psychotropic drugs (aspirin) and regular culture media. We observed that SNORD90 expression
120 was up-regulated exclusively by antidepressant drugs, while other treatments did not
121 significantly alter SNORD90 expression (figure 1E). Together our data suggests that
122 antidepressant treatment response associates with an increase in SNORD90 expression.

123

124 **SNORD90 over-expression in mouse ACC induces anti-depressive like behaviours**

125 Given that we observed an upregulation of SNORD90 with antidepressant treatment response in
126 humans and mice, we next investigated if the over-expression of Snord90 in the cg 1/2 cortex of
127 mice has behavioural implications. We over-expressed (OE) Snord90 or a full scrambled
128 Snord90 sequence control in the mouse cg1/2 via bilateral injections of an adeno-associated virus
129 (AAV) followed by a battery of behavioural tests designed to measure anxiety and depressive-

130 like behaviors in mice (figure 2A). We did not observe any differences in the total distance
131 traveled in the open field test, which indicated no general locomotor differences between
132 Snord90 OE and full scramble OE (figure 2B). Snord90 OE increased the amount of time spent
133 in the open arm and decreased the amount of time spent in the closed arm of the elevated plus
134 maze (figure 2C). Moreover, Snord90 OE increased time spent grooming after splashing with
135 10% sucrose solution and increased time spent struggling in the tail suspension test (figure 2D-
136 E). Lastly, we calculated an integrated emotionality Z-score by combining data from the elevated
137 plus maze, splash test, and tail suspension test (figure 2F). Overall, our results consistently
138 showed that over-expressing SNORD90 levels in *cg1/2* yielded decreased emotionality
139 indicative of a decrease in anxiety-like and depressive-like behaviours (figure 2F).

140

141 **SNORD90 directly down-regulates NRG3**

142 SNORD90 is subcategorized as an orphan snoRNA as it does not have any canonical rRNA,
143 snRNA, or tRNA targets (13). However, more recent studies have indicated that some snoRNAs
144 exhibit atypical functioning such as regulation of alternative splicing and modulating expression
145 of mRNA (14-16). Thus, we explored possible RNA targets for SNORD90 using the basic local
146 alignment (BLAST) search tool for base complementarity, and using the C/D box snoRNA target
147 prediction tool “PLEXY” (17). Using these in-silico methods we identified NRG3 as a putative
148 gene target for SNORD90 (figure 3A & supplementary table 4-5). More specifically, we
149 identified three predicted binding regions for SNORD90 on the NRG3 pre-mRNA (pre-NRG3)
150 (figure 3A & supplementary table 4-5). NRG3 is a growth factor that is part of the neuregulin
151 family and that is highly enriched in the brain and has been previously associated with
152 psychiatric phenotypes (18-20). To determine if SNORD90 regulates NRG3, we first assessed

153 NRG3 expression in the same human and mouse ACC samples, as well as in the neuronal
154 cultures described above (supplementary figure 2A-C). We observed a negative correlation
155 between SNORD90 and NRG3 in all three experimental contexts (supplementary figure 2D-F),
156 and interestingly, we observed the most significant differences in direction of fold-change
157 between SNORD90 and NRG3 expression in groups with antidepressant drug exposure
158 (supplementary figure 2G-I).

159

160 To further investigate the relationship between SNORD90 and NRG3, we over-expressed
161 SNORD90 in human neural progenitor cells (NPCs) and assessed the resulting effects on NRG3
162 expression (supplementary figure 3A-B). We constructed AAV vectors expressing wild-type
163 SNORD90 (SNORD90 OE), as well as two scrambled controls (supplementary figure 3A). The
164 first control had a scramble sequence in the central region of the SNORD90 transcript, where the
165 predicted complementary sequence to NRG3 lies (seed scramble OE) and the second control had
166 a full scramble of the entire SNORD90 transcript (full scramble OE) (supplementary figure 3A).
167 SNORD90 OE resulted in a ~50% decrease in NRG3 expression at both the mRNA and protein
168 levels (figure 3B and supplementary figure 3C). Seed scramble OE and full scramble OE did not
169 alter the expression of NRG3, indicating the region of predicted complementarity between
170 SNORD90 and NRG3 plays an important role in the ability of SNORD90 to down-regulate
171 NRG3 (figure 3B). We also measured the expression of pre-NRG3, since our in-silico
172 predictions indicated that SNORD90 is primarily interacting with intronic regions of pre-NRG3,
173 however, pre-NRG3 expression was not altered by SNORD90 OE or any of the scrambled
174 controls (supplementary figure 3D). We next examined the effects of SNORD90 knock-down
175 (KD) using antisense oligonucleotides (ASO) (supplementary figure 4A-B). We screened four

176 ASOs that target different regions of SNORD90 and selected the ASO achieving the best KD
177 (supplemental figure 4A-B). SNORD90 KD by approximately 55% resulted in a ~50%
178 upregulation of NRG3 expression (figure 3C). We again did not observe any significant changes
179 at the level of pre-mRNA expression (supplementary figure 4C). Finally, to further confirm the
180 importance of direct interaction between SNORD90 and NRG3, we designed target blockers
181 which have sequence complementarity to the predicted SNORD90 binding sites on pre-NRG3
182 (figure 3D). Target blockers were co-transfected with our SNORD90 OE vectors (figure 3D).
183 Interestingly, when each individual site was blocked, we observed a partial rescue of NRG3
184 expression (figure 3E). However, simultaneously blocking all three predicted sites was required
185 for a complete rescue of the downregulation effects of SNORD90 OE (figure 3E). Pre-NRG3
186 expression was not altered by any target blockers (supplementary figure 5). Together our data
187 suggests that SNORD90 directly down-regulates NRG3 expression through multiple interaction
188 sites on intronic regions.

189

190 **SNORD90 associates with RBM15B and guides m6A modifications onto NRG3**

191 We next asked what mechanisms may explain SNORD90's effects on NRG3 given that it
192 interacts with intronic regions of NRG3, and yet, it does not affect pre-mRNA levels of NRG3.
193 Since SNORD90 displays atypical functioning, we posited that it could regulate NRG3 through
194 the recruitment of a unique set of RNA binding proteins (RBPs) that is different from
195 canonically functioning C/D box snoRNAs (21). Using the in-silico tool "oRNament" we
196 identified a sequence-motif for RNA Binding Motif Protein 15B (RBM15B); this motif sequence
197 was further confirmed by Van Nostrand et al., 2020 (22, 23) (supplemental table 6). RBM15B is
198 a key regulator of RNA N6-methyladenosine (m6A) modifications by facilitating interactions

199 with Wilms' tumor 1-associating protein (WTAP), which in turn binds to methyltransferase like
200 3 (METTL3) forming a major m6A writer complex (24). To confirm the association of
201 SNORD90 with RBM15B, we performed RNA immunoprecipitation (RIP) against RBM15B as
202 well as the canonical core enzymatic protein for C/D snoRNAs, Fibrillarin (figure 4A) (25, 26).
203 We observed a significantly higher level of association of SNORD90 to RBM15B compared to
204 fibrillarin whereas a canonically functioning snoRNA, SNORD44, displayed enrichment for
205 fibrillarin IP (figure 4A). Furthermore, when we over-expressed SNORD90 we observed an
206 increase in association of SNORD90 with RBM15B, compared to over-expression of a
207 scrambled control (figure 4B). We did not observe an increase of SNORD90 association with
208 Fibrillarin following SNORD90 OE, indicating that SNORD90 showed preference for
209 interacting with RBM15B (figure 4B). Since snoRNAs and RBM15B are both found in the
210 nucleus this may in part explain SNORD90's role in interacting with intronic regions of NRG3
211 pre-mRNA (21, 24). Canonical snoRNAs function by guiding their partner proteins to target
212 transcripts which, in-turn, induce a chemical modification (27). Thus, we hypothesized that
213 SNORD90 is likely acting as a guide RNA for RBM15B and its associated m6A writer complex,
214 resulting in an increase in m6A levels on NRG3. To test this hypothesis, we measured total m6A
215 abundance on NRG3 and pre-NRG3 transcripts from our SNORD90 OE in-vitro NPC culture
216 experiments detailed above. We observed an increase of m6A abundance on both NRG3 and pre-
217 NRG3, following SNORD90 OE, whereas seed scramble OE and full scramble OE did not alter
218 m6A abundance (figure 4C-D). Furthermore, introducing target blockers blunted the increase of
219 m6A abundance on both NRG3 and pre-NRG3 (figure 4E-F). To further test RBM15B's role in
220 the observed increase in m6A levels on NRG3, we used dicer-substrate short interfering RNAs
221 (dsiRNAs) to knock-down RBM15B (RBM15B KD) (supplementary figure 6). RBM15B KD

222 followed by SNORD90 OE blunted the increase of m6A levels on NRG3 and pre-NRG3 (figure
223 4G-H). RBM15B KD also blunted the decrease of NRG3 expression following SNORD90 OE
224 (figure 4G-H). Interestingly we observed a significant negative correlation between m6A levels
225 and expression of NRG3, but this was not observed for pre-NRG3, which could possibly be
226 explained by the fact that m6A-readers are primarily located in the cytoplasm, and thus would
227 only recognize the m6A-modifications of the mature NRG3 transcript and promote its decay
228 when it is shuttled out of the nucleus into the cytoplasm (supplementary figure 7). Ke et al., 2017
229 demonstrated that m6A modifications are added onto nascent pre-mRNA during transcription
230 (28). Moreover, m6A levels remain unchanged between nascent pre-mRNA and steady-state
231 mRNA in the cytoplasm (28). Our results further support these findings as it is possible that
232 SNORD90 is guiding m6A modifications onto NRG3 at the pre-mRNA level, which are retained
233 in the mRNA molecule. Although it is unclear why SNORD90 targets intronic regions, while it
234 seems that m6A modifications are deposited onto exonic regions, this could perhaps be explained
235 by the secondary structure of the RNA molecule where exonic regions could be looping closer to
236 the SNORD90-guided methylation complex.

237

238 The YTH family of proteins are the best described readers of RNA m6A modifications. The
239 YTH family includes: YTHDF1, YTHDF2, YTHDF3, YTHDC1, and YTHDC2. Of these,
240 YTHDF1, YTHDF2 and YTHDF3 regulate RNA stability, whereas functional implications for
241 YTHDC1 and YTHDC2 are less well defined (29, 30). Furthermore, YTHDF1, YTHDF2,
242 YTHDF3, and YTHDC2 are primarily located in the cytoplasm, whereas YTHDC1 is primarily
243 located in the nucleus (31). We selectively knocked-down each of the above-mentioned m6A-
244 readers using dsRNAs followed by SNORD90 OE to elucidate which m6a-reader(s) are

245 involved in the down-regulation of NRG3 (figure 4I & supplementary figure 8). Although
246 YTHDF1 KD, YTHDF2 KD, and YTHDF3 KD all showed the ability to blunt the decreased
247 NRG3 expression following SNORD90 OE, YTHDF2 displayed the most robust ability to blunt
248 this effect, recovering NRG3 expression to WT patterns (figure 4I). On the other hand, YTHDC2
249 KD and YTHDC1 KD did not blunt the decrease of NRG3 expression after SNORD90 OE;
250 displaying similar patterns of NRG3 expression to SNORD90 OE with a dsRNA scramble
251 control (siControl) (figure 4I). Interestingly, YTHDC1 KD, the nuclear m6a-reader, resulted in a
252 decrease of pre-mRNA levels of NRG3 expression compared to WT, while knock-down of all
253 other m6a-readers had no significant effect on pre-NRG3 expression levels (supplementary
254 figure 9). Together this evidence supports the hypothesis that 1) SNORD90 increases NRG3
255 m6A transcript methylation and subsequent decay, and 2) that the decay occurs primarily in the
256 cytoplasm (figure 4J). This, in turn, explains why we only observed changes in NRG3 mRNA
257 and protein levels, but did not observe changes in pre-mRNA levels following SNORD90 OE.

258

259 **SNORD90 mediates down-regulation of Nrg3 resulting in increased glutamatergic** 260 **neurotransmission**

261 We next investigated the functional relevance of decreased NRG3 expression in-vivo. NRG3 has
262 previously been shown to interact with syntaxin, disrupting SNARE complex formation in the
263 presynaptic terminal, and inhibiting vesicle docking (19). Nrg3 knock-out resulted in increased
264 probability of glutamate release in mouse hippocampal neurons (19). To investigate if
265 SNORD90-mediated down-regulation of NRG3 has a similar effect in mice, we first investigated
266 if SNORD90's ability to down-regulate NRG3 is conserved in mice. We performed in-silico
267 target prediction between mouse Snord90 and Nrg3 using "PLEXY" (supplementary table 7).

268 Although predicted sequence complementary sites between Snord90 and Nrg3 are not as robust
269 as in humans, there is conservation between the two species (supplementary table 7 and
270 supplementary figure 10). To further explore this effect, we over-expressed Snord90 or a full
271 scrambled control in the mouse ACC (cg1/2) via bilateral injections of an AAV virus (figure
272 5A). RT-qPCR confirmed successful over-expression of Snord90 and subsequent down-
273 regulation of Nrg3 in mice (figure 5B). Next, we performed whole-cell patch-clamp recordings
274 from pyramidal neurons of the ACC in acute brain slices from mice over-expressing Snord90 or
275 the full scramble control. We observed an increase in spontaneous excitatory postsynaptic
276 currents (sEPSC) frequency following Snord90 OE compared to full scramble control without
277 any effect on sEPSC amplitude (figure 5C-E). This increase in glutamatergic neurotransmission
278 is likely due to an increase in glutamate release probably resulting from NRG3 pre-synaptic
279 expression and effect on SNARE complex (19). Together this indicates that SNORD90-mediated
280 down-regulation of NRG3 has implications in glutamate neurotransmission, which translates to
281 behavioral changes such as anxiolytic and anti-depressive-like behaviors.

282

283 **DISCUSSION:**

284 In this study, we demonstrated that SNORD90 mediates antidepressant drug action through
285 regulation of NRG3. While it is unclear how serotonergic antidepressant drugs may promote the
286 increase of SNORD90 expression, one possible mechanism may be through histone
287 serotonylation. Previous studies have demonstrated that serotonin can covalently attach to
288 histone H3 and influence gene expression (32). The administration of serotonergic
289 antidepressants could change intracellular monoamine levels influencing the expression of
290 SNORD90; however, future studies are needed to investigate this hypothesis. Our results indicate

291 that SNORD90 associates with RBM15B and is involved in mediating m6A modifications,
292 specifically onto NRG3. This is a slight but significant divergence from canonically functioning
293 C/D box snoRNAs that are known to associate with fibrillarin, a methyltransferase responsible
294 for 2'O-methylation (2'OMe) (33, 34). Whereas 2'OMe can occur on the ribose of any base and
295 is associated with increased RNA stability, m6A is an adenosine specific modification with a
296 diverse range of effects on RNA stability (31, 35). Specifically, our data show that increased
297 m6A levels elicit NRG3 decay through recognition by the m6A reader YTHDF2. Furthermore,
298 SNORD90's influence on NRG3 appears to bridge a relationship between the monoaminergic
299 and the glutamatergic systems. Many studies have shown that antidepressant drugs target the
300 monoaminergic system but also affect the glutamatergic system (9). However, it has not been
301 clear until now what is mediating these effects, though they have often been attributed to off
302 target binding of antidepressant drugs. Our study offers molecular evidence supporting one
303 particular mechanism that might mediate the link between serotonin targeting drugs and
304 activation of the glutamatergic system. Although NRG3 expression has been associated with
305 psychiatric disorders including MDD, it has not previously been associated with antidepressant
306 treatment (18). NRG3 is primarily expressed in excitatory pyramidal neurons, and accordingly,
307 the increase of SNORD90 in response to antidepressant treatment, can yield specific effects on
308 excitatory glutamatergic neurons and thus glutamatergic neurotransmission (19, 36). Gaining a
309 better understanding of the molecular mechanisms of antidepressant treatment response will
310 offer new targets for the development of more effective treatments of MDD.

311

312 **MATERIALS AND METHODS:**

313 **Human Clinical trial Subjects**

314 Three independent cohorts were used in this study, comprising 660 individuals (37-39).

315

316 Cohort 1 (N=258) was obtained in collaboration with Lundbeck A/S sponsored clinical trials and
317 is composed of individuals diagnosed with MDD in a current major depressive episode (MDE)
318 who were enrolled in a double-blind clinical trial and received treatment with either duloxetine
319 (60mg), a serotonin-norepinephrine reuptake inhibitor (SNRI), or placebo for eight weeks. For
320 each patient, peripheral blood samples were collected at baseline (T0) and after treatment (T8).
321 Participants, aged 19–74 years, were recruited based on a primary diagnosis of MDD and MDE
322 lasting at least 3 months, with a severity score on the Montgomery-Åsberg Depression Rating
323 Scale (MADRS) of ≥ 22 at T0. Participants resistant to at least two previous AD treatments or
324 who had received electroconvulsive therapy in the 6 weeks before the study began were
325 excluded. Other exclusion criteria included: MDE in bipolar disorder, presence of psychotic
326 features, and recent substance use disorder. This clinical trial was approved by ethics boards of
327 participating centers, and all participants provided written informed consent.

328 www.ClinicalTrials.gov (11984A NCT00635219; 11918A NCT00599911; 13267A

329 NCT01140906). For more details, please refer methods section of Lopez et al., 2017 (37).

330

331 Cohort 2 (N=236) was obtained in collaboration with the Canadian Biomarker Integration
332 Network in Depression (CAN-BIND) and is composed of individuals diagnosed with MDD
333 (N=153) and healthy controls (N=83). Patients and controls were recruited at six Canadian
334 clinical centers. Exclusion criteria included personal and family history of schizophrenia or
335 bipolar disorder, or current substance dependence. Depressed patients were treated with
336 escitalopram (10-20mg per day), a selective serotonin reuptake inhibitor (SSRI), for eight weeks.

337 Depression severity was assessed at baseline and after treatment by MADRS. This trial was
338 approved by ethics boards of participating centers and all participants provided written informed
339 consent. www.ClinicalTrials.gov identifier NCT01655706. Registered 27 July 2012. For more
340 details, please refer to Kennedy et al., 2019 (38).

341
342 Cohort 3 (N=166) was obtained at the Douglas Mental Health University Institute and is
343 composed of healthy controls (N=28) and individuals diagnosed with MDD (N=138) who were
344 enrolled in the community outpatient clinic at the Douglas Mental Health University Institute.
345 Depressed patients were treated with either desvenlafaxine, a serotonin-norepinephrine reuptake
346 inhibitor (SNRI) or escitalopram, a selective serotonin reuptake inhibitor (SSRI). For each
347 patient, a blood sample was taken at baseline before treatment administration and 8 weeks post-
348 treatment. Participants (healthy controls and individuals with MDD) were excluded from the
349 study if they had comorbidity with other major psychiatric disorders, if they had positive tests for
350 illicit drugs at any point during the study, or if they had general medical illnesses. Individuals
351 with MDD were not receiving antidepressant treatment at the onset of the trial, and received a
352 diagnosis of MDD without psychotic features, according to the Statistical Manual of Mental
353 Disorders, Fourth Edition (DSM-IV). Control subjects were excluded if they had a history of
354 antidepressant treatment. Eligible participants were randomized to either desvenlafaxine (50-
355 100mg) or escitalopram (10-20mg) treatment. All subjects included in the study provided
356 informed consent, and the project was approved by The Institutional Review Board of the
357 Douglas Mental Health University Institute. For more details, please refer to Jollant et al., 2020
358 (39).

359

360 ***Clinical Assessment***

361 All participants from all cohorts were assessed for depression severity after 6 to 8 weeks of
362 treatment. To quantify treatment response, we calculated percentage change of MADRS scores
363 (from baseline to after treatment). We used percentage change to correct for the potential effects
364 of differential baseline scores. Additionally, we classified participants as responder/non-
365 responder based on >50% decrease in MADRS scores from baseline.

366

367 ***Human peripheral blood sample processing and RNA Extraction***

368 Peripheral blood samples from cohort 1 were collected in PAXgene blood RNA tubes
369 (PreAnalytix). Total RNA was isolated from whole blood using the PAXgene Blood miRNA Kit
370 (Qiagen, Canada) according to the manufacturer's instructions. Peripheral blood samples from
371 cohort 2 and cohort 3 were collected in EDTA blood collection tubes and passed through
372 LeukoLOCK filters (ThermoFisher) to capture the total leukocyte population, eliminating red
373 blood cells, platelets, and plasma. Filters, containing leukocytes, were frozen at -80C for storage
374 until ready for sample processing. Total RNA was extracted using a modified version of the
375 LeukoLOCK Total RNA Isolation System protocol (ThermoFisher). All samples were treated
376 with DNase digestion during RNA purification using the RNase-Free DNase kit (Qiagen). RNA
377 yield and quality were determined using the Nanodrop 1000 (Thermo Scientific, USA) and
378 Agilent 2200 TapeStation (Agilent Technologies, USA).

379

380 ***Library Construction and Small RNA-Sequencing***

381 Libraries for cohort 1 and cohort 3 were prepared using the Illumina TruSeq Small RNA
382 protocol following the manufacturer's instructions. Libraries for cohort 2 were prepared using

383 NEB small RNA protocol following manufacturer's instructions. All libraries were purified
384 using biotinylated magnetic AMPure beads that allow for selection of specified complementary
385 cDNA products bound to streptavidin. A total of 50µl of amplified cDNA were mixed and
386 purified twice with AMPure XP beads in a 1.8:1 ratio (beads/sample). Cohort 1 was sequenced
387 using Illumina HiSeq2500, cohort 2 was sequenced using Illumina HiSeq4000, and cohort 3 was
388 sequenced using Illumina HiSeq2000. All samples were sequenced at the McGill University and
389 Genome Quebec Innovation Centre (Montreal, Canada) using 50 nucleotide single-end reads. All
390 sequencing data was extracted from FASTQ files and processed using CASAVA 1.8+. Illumina
391 adapter sequences were trimmed using the Fastx_toolkit, and additionally filtered by applying
392 the following cut-offs: (1) Phred quality (Q) score higher than 30, (2) reads between 15-40nt in
393 length, (3) adapter detection based on perfect-10nt match, and (4) removing reads without
394 detected adapters. Bowtie35 (John Hopkins University) was used to align reads to the human
395 genome (GRCh37). Furthermore, Rfam database was used to map reads to known small
396 nucleolar RNAs. Sequencing data was normalized with the Bioconductor-DESeq2 package.

397

398 *Statistical analysis*

399 For each subject in these trials, samples collected before administration of an antidepressant (T0)
400 and eight weeks following antidepressant treatment (T8) were analyzed according to response to
401 treatment based on MADRS score changes. For the discovery cohort, antidepressant treated, and
402 placebo treated subjects were analyzed separately.

403

404 A two-way mixed multivariable analysis of variance (2WM-MANOVA) was used to identify
405 snoRNAs that had a significant interaction between treatment response (response/non-response)

406 and treatment course (T0/T8). For cohort 1, antidepressant treated, and placebo treated subjects
407 were analyzed separately. All detected snoRNAs were assessed in cohort 1. Only snoRNAs that
408 showed significant interactions were assessed in cohort 2 and subsequently only snoRNAs that
409 were replicated in cohort 2 were assessed in cohort 3. For all cohorts, outliers were identified
410 using boxplot methods with values above quartile 3 (Q3) + 1.5 interquartile range (IQR) or
411 below quartile 1(Q1) - 1.5IQR (IQR=Q3-Q1). Shapiro-Wilk test and QQ plots were used to
412 assess data normality. All above mentioned tools were apart of publicly available R package
413 “rstatix” (<https://CRAN.R-project.org/package=rstatix>) (40).

414

415 **Unpredicted chronic mild stress (UCMS) mouse model:**

416 Eight-week old male BALB/c mice (N=23; Centre d’Elevage Janvier, Le Genest St. Isle, France)
417 were divided into four groups as described by Herve et al., 2017 (12). In brief, control group (N
418 = 5) was kept in standard housing conditions for 8 weeks. UCMS only group (N = 7) comprised
419 of mice subjected to the Unpredictable Chronic Mild Stress (UCMS) procedure for 8 weeks.
420 UCMS-flx group (N=5) included mice that were subjected to the UCMS procedure for 8 weeks
421 and treated in parallel by fluoxetine (flx) during the last 6 weeks. Flx only group (N = 6)
422 included mice that did not undergo the UCMS procedure but were treated with fluoxetine during
423 the last 6 weeks. Mice from the control and flx only groups were housed in standard cages,
424 whereas the UCMS-exposed mice were isolated in individual home cages with no physical
425 contact with other mice. The stressors used were varied and applied in a different sequence each
426 week to avoid habituation.

427

428 Stressors consisted of housing on damp sawdust (about 200 mL of water for 100 g of sawdust),
429 sawdust changing (replacement of the soiled sawdust by an equivalent volume of new sawdust),
430 placement in an empty cage (usually the home cage of the subject, but with no sawdust),
431 placement in an empty cage with water (the mouse is placed in its empty cage, whose bottom has
432 been filled up with 1 cm high water at 21°C), switching cages (also sometimes termed as social
433 stress: the mouse from a cage A is placed in the soiled cage from mouse B, mouse B itself being
434 absent in order to avoid aggressive interactions), cage tilting (45°), predator sounds, introduction
435 of rat or cats feces as well as fur in the mouse home cage, inversion of the light/dark cycle, lights
436 on for a short time during the dark phase or light off during the light phase, confinement in small
437 tubes (diameter: 4 cm; length: 5 cm).

438

439 ***Mice Behavior***

440 Weight and coat state were measured weekly, as markers of UCMS-induced depressive-like
441 behavior, except for the last week before sacrifice, when coat state from seven different areas of
442 the body was recorded twice, separated by 3-day intervals. At the end of the 8th week, a
443 complementary test of nest building was performed just before sacrifice. The test was
444 administered by isolating mice in their home cages. For additional details please refer to Herve et
445 al., 2017 (12).

446

447 ***Quantification and statistical analysis***

448 Details related brain dissection and RNA extraction can be found at Herve et al., 2017 (12). RNA
449 was reverse-transcribed using M-MLV Reverse Transcriptase (200 U/μL) (ThermoFisher) with
450 random hexamers. SNORD90 and NRG3 were quantified by RT-PCR using SYBR green

451 (Applied Biosystems). Reactions were run in triplicate using the QuantStudio 6 Flex System and
452 data collected using QuantStudio Real-Time PCR Software v1.3. One-way ANOVA was used as
453 described above.

454

455 **Human Post-Mortem Brain**

456 Post-mortem samples of dorsal ACC (Brodmann Area 24) were obtained, in collaboration with
457 the Quebec Coroner's Office, from the Douglas-Bell Canada Brain Bank (Douglas Mental
458 Health University Institute, Montreal, Quebec, Canada). Groups were matched for post-mortem
459 interval (PMI), pH and age. Psychological autopsies were performed as described previously,
460 based on DSM-IV criteria (41). The control group had no history of major psychiatric disorders.
461 All cases met criteria for MDD or depressive disorder not-otherwise-specified. Written informed
462 consent was obtained from next-of-kin. This study was approved by the Douglas Hospital
463 Research Centre institutional review board.

464

465 ***RNA-sequencing***

466 RNA was extracted from all brain samples using a combination of the miRNeasy Mini kit and
467 the RNeasy MinElute Cleanup kit (Qiagen), with DNase treatment, and divided into small
468 (<200 nt) and large (>200 nt) fractions. RNA quality, represented as RNA Integrity Number, was
469 assessed using the Agilent 2200 TapeStation. Small RNA-seq libraries were prepared from the
470 small RNA fraction, using the Illumina TruSeq Small RNA protocol following the
471 manufacturer's instructions. Samples were sequenced at the McGill University and Genome
472 Quebec Innovation Centre (Montreal, Canada) using the Illumina HiSeq2000 with 50nt single-
473 end reads. All sequencing data were processed using CASAVA 1.8 + (Illumina) and extracted

474 from FASTQ files. The Fastx_toolkit was used to trim the Illumina adapter sequences.
475 Additional filtering based on defined cutoffs was applied, including: (1) Phred quality (Q) mean
476 scores higher than 30, (2) reads between 15 and 40 nt in length, (3) adapter detection based on
477 perfect-10nt match, and (4) removal of reads without detected adapter. In addition, we used
478 Bowtie [24] to align reads to the human genome (GRCh37). Furthermore, all sequencing data
479 was normalized with the Bioconductor—DESeq2 package, using a detection threshold of 10
480 counts per snoRNA. We retained all snoRNAs with >10 reads in 70% of either group (controls,
481 cases) for differential analyses. RNA extractions, sequencing, and data processing were
482 conducted by blinded investigators. For additional details please refer to Fiori et al., 2020 (42).
483

484 *Statistical analysis*

485 Using toxicology screens, each sample was separated into the following groups: MDD with
486 presence of antidepressants, MDD with presence of non-antidepressant drugs, MDD with
487 negative toxicology screen, controls with non-antidepressant drugs, and controls with negative
488 toxicology screens. No control samples were positive for antidepressant drugs. For this analysis
489 we only investigated the expression for SNORD90 from this small RNA sequencing dataset.
490 NRG3 was measured via qPCR from cDNA converted from the same RNA aliquot for each
491 sample. Analysis was performed in R using “rstatix” as mentioned above employing a one-way
492 ANOVA. Shapiro-Wilk test and QQ plots were used to assess data normality.

493

494 **Human hindbrain NPC Culture and neuronal differentiation**

495 Monoamine producing neurons were generated from human induced pluripotent stem cells
496 (iPSCs), using a protocol adapted from Lu et al. 2016 (43). Human iPSCs were first cultured in

497 DMEM/F12 (Gibco) supplemented with N2 (Gibco), B27 (Gibco), nonessential amino acids
498 (Gibco), 1% GlutaMAX (Gibco), 2 uM SB431542 (STEMCELL Tech.), 2uM DMH1 (Tocris),
499 and 3uM CHIR99021 (Tocris); collectively referred to as SDC media. Culturing in SDC media
500 for 1 week induces human iPSC differentiation into rostral hindbrain neural stem cells (NSCs).
501 Rostral hindbrain NSCs colonies were selected and re-plated in SDC media supplemented with
502 1000 ng/ml of SHH C25II (GenScript). Hindbrain NPCs were GBX2, HOXA2, and HOXA4
503 positive as assessed via quantitative RT-PCR to confirm hindbrain specificity at this
504 developmental stage. Ventral rostral hindbrain NSC colonies were collected and re-plated in
505 SDC + SHH media along with 10ng/ml of FGF4 (PeproTech). SDC + SHH + FGF4 media will
506 induce ventral rostral hindbrain NSC differentiation into neural progenitor cells (NPCs) after 1
507 week. NPCs were expanded in SDC+SHH+FGF4 media and differentiated into monoamine
508 producing neuron-like cells. NPCs were differentiated, for 1 month, into neuron-like cells in
509 neurobasal media (Gibco) supplemented with N2, B27, NEAA, 1ug/ml laminin (Sigma), 0.2mM
510 vitamin C (Sigma), 2.5uM DAPT (Sigma), 10ng/ml GDNF (GenScript), 10ng/ml BDNF
511 (GenScript), 10ng/ml insulin-like growth factor-I (Pepro Tech), and 1ng/ml transforming growth
512 factor β 3 (Pepro Tech). Post-differentiation, neuron-like cells underwent high-performance
513 liquid chromatography (HPLC) to test for monoamine production. HPLC confirmed production
514 of norepinephrine (NE), epinephrine (epi), dopamine (DA), and serotonin (5-HT). All NPCs and
515 differentiated NPCs were seeded on culture plates coated with 100ug/mL poly-L-ornithine
516 (sigma) and 10ug/mL laminin (Sigma) and grown in a 5% CO₂ humidified incubator at 37°C.

517

518 ***High Performance Liquid Chromatography***

519 Cells were sonicated in 60uL of 0.25 N perchloric acid. Protein and cellular debris were cleared
520 by centrifugation at 11,000g at 4°C for 10 min. Pellets were re-suspended in 100µl of 0.1N
521 NaOH. 20uL of tissue homogenates, cleared of protein and debris, was injected using a
522 refrigerated ultimate 3000 rapid separation autosampler (ThermoFisher) into a HPLC system
523 consisting of a luna 3 u C18 (2) 100 A 75 X 4.6 mm phenomemex and a coulometric
524 electrochemical detector (ThermoFisher) to quantify monoamines. Oxidation and reduction
525 electrode potentials of the analytical cell (5014B; ThermoFisher) were set to +300 and -250 mV
526 respectively. The mobile phase consisting of 73.4mM sodium acetate trihydrate, 66.6mM of
527 citric acid monohydrate, 0.025mM Na₂EDTA, 0.341mM 1-octanesulfonic acid, 0.71mM of
528 Triethylamine and 6% (v/v) methanol (pH adjusted to 4.0-4.1 with acetic acid) was pumped at
529 1.5 ml/min by a solvent delivery module (dionex ultimate 3000 rs pump).

530

531 **NPC Drug Treatment**

532 Human NPCs were screened for cytotoxic effects using the MTT assay, and antidepressants were
533 applied at nontoxic concentrations as described by Lopez et al., 2014 (44). NPCs were cultured
534 in 24 well plates and differentiated, for 2 weeks, into neuron-like cells in neurobasal media
535 (Gibco) supplemented with N2, B27, NEAA, 1 µg/ml laminin (Sigma), 0.2 mM vitamin C
536 (Sigma), 2.5 µM DAPT (Sigma), 10 ng/ml GDNF (GenScript), 10 ng/ml BDNF (GenScript),
537 10 ng/ml insulin-like growth factor-I (Pepro Tech), and 1 ng/ml transforming growth factor β3
538 (Pepro Tech). Following 2 weeks of differentiation, culture media was supplemented with
539 escitalopram (Sigma-Aldrich, E4786; 100 µM), duloxetine (Sigma-Aldrich, Y0001453; 10 µM),
540 haloperidol (Sigma-Aldrich, H1512; 10 µM), lithium (Sigma-Aldrich, L4408; 1 mM), Aspirin
541 (Sigma-Aldrich, A5376; 1mM), or left untreated (controls). Cells for each drug treatment were

542 incubated for 48 h before harvest and RNA extractions. Each drug treatment was performed in
543 triplicate. RNA was extracted using the Zymo DirectZol RNA Extraction kit. cDNA construction
544 and RT-qPCR were as described above. One-way ANOVA analysis was performed in IBM
545 SPSS Statistics version 27 using Dunnett's post-hoc correction.

546

547 **SNORD90 over-expression in mice:**

548 Male CD-1 (ICR) were housed in temperature-controlled ($23 \pm 1^\circ\text{C}$), constant humidity ($55 \pm$
549 10%), 12-hour light/dark cycle and in specific-pathogen-free conditions. Animals had access to
550 food and water *ad libidum*. Animals were housed in groups of four. All animal experiments were
551 evaluated and approved by the local commission for the Care and Use of Laboratory Animals of
552 the Government of Upper Bavaria, Germany.

553

554 ***Cloning***

555 The Snord90 sequence was obtained from the Ensembl genome browser database (Ensemble ID
556 ENSMUSG00000077756). The control sequence was generated by scrambling the Snord90 gene
557 using siRNA wizard software (Invitrogen). Each fragment was designed to have KpnI and
558 BamHI and a 10-nucleotide long overhang with the vector backbone at the 5' and 3' ends
559 respectively. Each gene fragment was inserted into a KpnI with BamHI linearized pAAV-EF1a-
560 eGFP-H1 backbone using Gibson Assembly (NEB) according to the manufacturer's protocol.
561 This generated the following two vectors, pAAV-EF1a-eGFP-H1-Scramble and pAAV-EF1a-
562 eGFP-H1-Snord90. All plasmids were checked for mutations by DNA sequencing.

563

564 SNORD90 sequence (mouse):

565 5'AAATAATGTTTTTAAGTGTCTAGTGATGAATTCATAGGGCAGATTCTGAGGTGAA
566 AATTTAGTTCATCATTGATTGTCCTATTATGAAATCTGAAGACACTTGAAAATA 3'

567

568 Scrambled sequence (mouse):

569 5'GATATTATAACGATTGTTGTATAATCTATTAGAGTGTATCGTAGGCAATGGCTATA
570 TGTAATGTAACGTATTGTACTCGTATGATTAATTACATAATACGAATACGCTAG 3'

571

572 *Validation of constructs*

573 Mouse neuroblastoma neuro2a (N2a) cells were maintained at 37°C with 5% CO₂ in Minimum
574 Essential Medium (MEM), 1x Glutamax, supplemented with 1x non-essential amino acids, 1mM
575 sodium pyruvate, 100 U/ml penicillin, 100 µg/ml streptomycin and 10% fetal bovine serum
576 (FBS, Gibco). Cells were detached with trypsin and transfected using ScreenfectA (ScreenFect
577 GmbH) according to the manufacturer's protocol. Cells were fixed with 4% PFA-PBS solution
578 and embedded with Fluoromount-G mounting medium containing DAPI (SouthernBiotech).
579 Cells were imaged using an Axioplan 2 fluorescent microscope (Zeiss).

580

581 *Virus production*

582 Human embryonic kidney cells (HEK293) were cultured in Dulbecco's Modified Eagle Medium
583 (DMEM) supplemented with 10% FBS, 100 U/ml penicillin and 100 µg/ml streptomycin
584 (Invitrogen) in a 5% CO₂ humidified incubator at 37°C. Cells were transfected with the gene
585 transfer rAAV plasmid combined with the helper plasmids in an equal molar ratio of 1:1:1 using
586 1 mg/ml linear polyethylenimine hydrochloride (PEI). The rAAV (serotype 1/2) particles were
587 harvested three days after transfection by lysing the cells with three consecutive freeze-and-thaw

588 cycles using an ethanol on dry ice bath and 37°C water bath. Lysates were centrifuged (3000 rcf)
589 followed by purification of the rAAV particles using a Heparin Agarose Type I chromatography
590 column (Sigma). The eluted rAAV particles were PBS washed using a 100000 MWCO Amicon
591 Ultra Filter (Millipore) and suspended in a final volume of 100µl. The number of viral genomic
592 particles was determined using quantitative RT-PCR resulting in the following titers; AAV1/2-
593 EF1a-eGFP-H1-Scramble $1,67 \times 10^{11}$ genome particles (gp)/µl and AAV1/2-EF1a-eGFP-H1-
594 Scramble 5×10^{10} gp/µl.

595

596 *Stereotactic surgery*

597 Eight-week-old mice were anesthetized with isoflurane and placed in the stereotactic apparatus
598 (TSE Systems) on a 37°C heating pad. Pre-surgery, mice were given Novalgine (200 mg/kg body
599 weight) and Metacam (sub-cutaneous 0.5 mg/kg body weight). During surgery, mice were
600 continuously supplied with 2% v/v isoflurane in O₂ through inhalation. Viruses were injected
601 bilaterally using a 33-gauge injection needle with a 5 µl Hamilton syringe coupled to an
602 automated microinjection pump (World Precision Instruments). Virus was delivered at a rate of
603 0.1 µl/min, to inject 0.25 µl for behavior experiments, and 0.5 µl for molecular experiments. The
604 injection coordinates were determined using the Franklin and Paxinos mouse brain atlas, from
605 bregma: ML +/-0.3 mm bilateral; AP +1.2 mm; DV -1.8 mm. After injection the needle was
606 retracted 0.01 mm and kept at the site for 2.5 minutes, followed by slow withdrawal. In all
607 experiments, each group consisted of two scramble control virus injected and two Snord90
608 overexpression virus injected animals. After surgery, the animals received Metacam for the 3
609 following days (intraperitoneal 0.5 mg/kg body weight). In all experiments, mice were tested or
610 tissue was extracted 3-4 weeks after surgery. After completion of the experiments, mice were

611 sacrificed by isoflurane overdose. For imaging of brain material, the brains were removed and
612 fixed in 4% PFA-PBS followed by dehydration in 30% sucrose-PBS solution for at least 24
613 hours each. Brains were sectioned (50 μm) using a vibratome (HM 650 V, Thermo Scientific).
614 Brain slices were imaged using the VS120-S6-W slide scanner microscope (Olympus). Injection
615 sites were verified based on green fluorescent protein (GFP) expression. For RNA extraction, the
616 brains were extracted and snap-frozen using methylbutane. Brains were sectioned in 200 μm
617 thick slices in a cryostat and the injection site was collected using 0.8 mm thick puncher. The
618 tissue was stored at -80°C until RNA extraction.

619

620 ***Real-time PCR (RT-PCR)***

621 Total RNA was extracted from cells or tissue using the miRNeasy Mini Kit (Qiagen). cDNA was
622 generated using the high-capacity cDNA RT kit with RNase inhibitor (Applied Biosystems)
623 according to the supplied protocol. RT-PCR was performed according to the manufacturer's
624 instructions using the QuantiFast SYBR green PCR Kit (Qiagen). RT-PCR data was collected on
625 the QuantStudio 7 Flex Real-Time PCR System (Applied Biosystems). Absolute expression
626 differences were calculated using the standard curve method. See supplementary table 8 for a list
627 of primer sequences used.

628

629 ***Behavioral tests***

630 For all behavioral tests, animals were brought into the room 30 minutes prior to the start of the
631 test to habituate the animals to the test room.

632

633 Open field (OF) test: The OF test was performed in a 50 x 50 cm light grey box, evenly
634 illuminated with low light conditions (<10 lux). Mice were placed in the open field facing one of
635 the walls and recorded for 6 minutes. Animals were tracked using ANY-maze software
636 (Stoelting). Total distance traveled was used as measure of animal locomotion.

637
638 Elevated plus maze (EPM): EPM apparatus was made of light grey material, and consists of four
639 intersecting arms elevated approximately 30 cm above the floor. The two opposing open (27.5 x
640 5 cm) and closed arms (27.5 x 5 x 20 cm) are connected with a central zone (5 x 5 cm). The
641 animals were placed in the center of the EPM, facing one of the open arms and recorded for 6
642 minutes. The closed arms were illuminated with <10 lux, while the open arms were illuminated
643 with 25-30 lux. Recordings were tracked and analyzed with ANYmaze software. Total time
644 spent in the open or closed arms was used as an anxiety measure.

645
646 Splash test (Spl): Animals were placed in a novel cage containing fresh bedding material and
647 were allowed to explore for 5 minutes. Each animal received two sprays of room temperature
648 10% sucrose water at the rear of their body. Animals were recorded for 6 minutes under low-
649 light conditions (<10 lux). The total groom time within the 3-6 minute timeframe was manually
650 scored using Solomon Coder software.

651
652 Tail suspension test (TST): In the TST, animals were taped by their tails on a metal rod,
653 approximately 30 cm above the ground, and illuminated with 30-35 lux. Animals were recorded
654 for 6 minutes and struggle time was quantified using ANY-maze software. The total time an

655 animal struggled within the 3-6 minute timeframe was used as a measure of a depression-like
656 emotional state.

657
658 Z-scoring was used to integrate multiple behavioral tests as previously described (45). First, the
659 z-score of each individual behavioral parameter was calculated.

660

$$z = \frac{X - \mu}{\sigma}$$

661
662 The z-scores of the EPM open arm, EPM closed arm, Spl and TST were combined to calculate
663 an integrated emotionality score.

664

$$Emotion\ z\ score = \frac{Z_{EPM} + Z_{Spl} + Z_{TST}}{Number\ of\ tests}$$

665
666 The final integrated score is associated with anxiety and depressive-like behaviors with a higher
667 score indicating a higher emotional state, while a lower score indicating a lower emotional state.

668

669 **Target Prediction**

670 The entire sequence of SNORD90 was used to blast against the human genome allowing G-T
671 wobble base pairing and one mismatch base pairing (supplemental table 4). Additionally, the
672 C/D box snoRNA target prediction algorithm PLEXY, using default parameters, was used for
673 target prediction of SNORD90 (17). SNORD90 mature sequence was used as the input snoRNA
674 and target sequence input was the entire human transcriptome using both mRNA and pre-mRNA

675 sequences downloaded from the Ensembl genome browser database (supplementary table 5).

676 Prediction was conducted using whole transcriptomics as well as a targeted analysis for NRG3.

677

678 **SNORD90 in-vitro knock-down**

679 SNORD90 was knocked down using antisense oligonucleotides (ASO) containing 2'-O-

680 methylations and phosphorothioate-modified nucleotides (supplementary table 9). Four ASOs

681 and one scrambled control ASO were screened to identify which achieved the best knock-down

682 of SNORD90 (supplementary figure 4). NPCs were plated in 24-well plates until ~90%

683 confluent before transfection with ASO (50nM final concentration) using Lipofectamine 2000

684 (ThermoFisher) following manufacturer's protocol. NPCs were incubated for 48 hours before

685 harvesting for RNA extraction. RNA extraction, cDNA synthesis, and RT-qPCR were as

686 described above. One-way ANOVA was used as described above

687

688 **SNORD90 in-vitro over-expression**

689 Constructs and cloning were as described above with the following sequences:

690 SNORD90 sequence:

691 5'TTATAAGTTTTCTAAGTGTCTAATGATGAATTTTCATAGGGCAGATTCTGAGGTGAA

692 AATTTAATTCATCACTGATACTCCTACTGTGGAATCTGAAGACACTTGAAAACGT 3'

693

694 Seed Scrambled sequence:

695 5'TTATAAGTTTTCTAAGTGTCTAATGATGAATTTTCATAGGGCAGATTCTGAAATAAT

696 ACTTCGCTTAAGATATTCGACTCCTACTGTGGAATCTGAAGACACTTGAAAACGT 3'

697

698 Scrambled sequence:

699 5'**GATTCATAATGAGTTGATTTAATCACATGCTGGCTCTCATTTCGACCAGAATTTCTCT**
700 **AGTTGATAAAAAGTAAACCAATGAATTAGTATGTTTGATCAAGATGTATGACTCG** 3'

701

702 NPCs were plated in 24-well plates until ~90% confluent before being transfected with each
703 vector using Lipofectamine 2000 (ThermoFisher) following manufacturer's protocol. NPCs were
704 incubated for 48 hours before harvesting for RNA extraction. RNA extraction, cDNA synthesis,
705 and RT-qPCR were as described above. One-way ANOVA was used as described above.

706

707 ***Target Blockers***

708 Modified RNA oligos containing 2'-O-methylations and phosphorothioate-modified nucleotides
709 (target blockers) were designed against three regions on the NRG3 transcript where SNORD90 is
710 predicted to bind (Figure 3A). Target blockers were co-transfected (30nM final concentration)
711 with SNORD90 OE vectors using lipofectamine 2000 following manufacturer recommendations
712 for "plasmid DNA and siRNA" co-transfection. For groups where target blockers were pooled
713 together, equal amounts for each target blocker were used totaling 30nM final concentration.
714 NPC culture conditions, RNA extraction, cDNA synthesis, and RT-qPCR were as described
715 above. One-way ANOVA was used as described above.

716

717 **Western blot**

718 Cell pellets from cell culture were lysed in lysis buffer [150 mM NaCl, 50 mM HEPES (pH 7),
719 50 mM EDTA, and 0.1% NP-40] and quantified using PierceTM BCA Protein Assay Kit (Thermo
720 Fisher). Equal amounts of proteins were electrophoresed on 4-20% Mini-PROTEAN TGX Stain-

721 Free Gels (Bio Rad). Proteins were then transferred onto nitrocellulose membranes using the
722 Trans-Blot Turbo Transfer System (Bio Rad). The membranes were blocked with 5% Bovine
723 Serum Albumin (BSA) in Phosphate-Buffered Saline (0.05% Tween 20) (PBS-T) at room
724 temperature for 1-2 hrs and then incubated with primary antibody (NRG3 (ab109256) at 1:500
725 and GAPDH (3683S) at 1:1000) in 1% BSA in PBS-T overnight at 4 °C. They were then
726 incubated with either biotin-conjugated anti-rabbit antibody (BA-1000) or with Horseradish
727 Peroxidase (HRP)-conjugated anti-rabbit antibody diluted 1:5000 in 1% BSA in PBS-T for 1 hr
728 at room temperature. The membranes that were incubated with biotin-conjugated anti-rabbit
729 antibody were washed with PBS-T and incubated with streptavidin-conjugated HRP (016-030-
730 084) at 1:5000 in 1% NFDM in PBS-T for 1 hr at room temperature. After washing,
731 immunoreactivity was detected using enhanced chemiluminescence solutions (ECL) and the
732 Biorad ChemiDocTM MP imaging system. Western blots were performed in 3 biological
733 replicates.

734

735 **RNA immunoprecipitation**

736 Overexpression of SNORD90 and scramble were performed as described above. RNA
737 immunoprecipitation (RIP) was performed using the Magna RIP RNA-Binding Protein
738 Immunoprecipitation kit (Millipore Sigma) following the manufacturer's protocol with slight
739 modifications. NPCs were collected and lysed in complete RIP lysis buffer. 10 uL of cell extract
740 was stored at -80°C and used as input. NPC extracts were incubated in RIP buffer containing
741 magnetic beads conjugated to anti-fibrillarin antibody (ab226178; abcam), anti-RBM15B
742 antibody (22249-1-AP; proteintech), or IgG control (provided by the kit) overnight in 4°C. Bead
743 complexes were washed 6 times with RIP buffer and eluted directly in TRIzol. RNA from all

744 conditions were purified in parallel using the RNA microPrep kit (Zymol) and eluted into 15 μ L
745 H₂O. The entire eluate was transcribed to cDNA using M-MLV Reverse Transcriptase
746 (200 U/ μ L) (ThermoFisher) with random hexamers. RT-qPCR was as described above.

747

748 **m6A-RIP**

749 m6A-RIP protocol was as described by Engel et al., with minor modifications. 3 μ g total RNA
750 was mixed with 3 fmol spike-in and equally split into 3 conditions: m6A-RIP, IgG control and
751 input. Input samples were frozen and kept at -80C during the m6A-RIP protocol. m6A-RIP and
752 IgG control samples were incubated with 1 μ g anti-m6A antibody (rabbit polyclonal 202 003,
753 Synaptic Systems) or 1 μ g normal rabbit IgG (NEB) in immunoprecipitation (IP) buffer (10 mM
754 Tris-HCl [pH 7.5], 150 mM NaCl, 0.1% IGEPAL CA-630 in nuclease-free H₂O, 0.5 mL total
755 volume) with 1 μ L RNasin Plus (Promega) rotating head over tail at 4°C for 2 hrs, followed by
756 incubation with 2x washed 25 μ L Dynabeads M-280 (Sheep anti-Rabbit IgG Thermo Fisher
757 Scientific) rotating head over tail at 4°C for 2 hrs. Bead-bound antibody-RNA complexes were
758 recovered on a magnetic stand and washed in the following order: twice with IP buffer, twice
759 with high-salt buffer (10 mM Tris-HCl [pH 7.5], 500 mM NaCl, 0.1% IGEPAL CA-630 in
760 nuclease-free H₂O), and twice with IP buffer. RNA was eluted directly into TRIzol and input
761 RNA was also taken up in TRIzol. RNA from all conditions was purified in parallel using the
762 RNA microPrep (Zymol) and eluted into 15 μ L H₂O. The entire eluate was transcribed to cDNA
763 using M-MLV Reverse Transcriptase (200 U/ μ L) (ThermoFisher) with random hexamers. RT-
764 qPCR was as described above. One-way ANOVA was used as described above

765

766 ***Spike-in***

767 A spike-in Oligo was used as a normalizer for quantitative RT-PCR. The spike-in oligo was
768 100nt in length with 3 internal m6A/m sites within GGAC motif flanked by the most frequent
769 nucleotides 5' U/A, 3' A/U, not complementary to hsa or mmu RefSeq mRNA or genome,
770 secondary structure exposing m6A sites (as described by Engel et al., 2018). The sequence is:
771 GCAGAACCUAGUAGCGUGUGGmACACGAACAGGUAUCAUAUGCGGGUAUGGmA
772 CUAAGCAACGUGCGAGAUUACGCUGAGGmACUACAAUCUCAGUUACCA
773 (synthesized by Horizon Discoveries).

774

775 **Dicer-Substrate Short Interfering RNA (dsiRNA) gene silencing**

776 DsiRNAs KD was assessed via RT-qPCR in the final experimental samples (supplementary
777 figure 8). In each silencing condition, the siRNA sequences were specific to the m6a reader of
778 interest, as shown by the quantitative RT-PCR data (supplementary figure 8). Cells were seeded
779 in 24-well plates and grown to ~70% confluency. 50nM siRNA was transfected using
780 lipofectamine 2000 according to the manufacturer's instructions. A second transfection was
781 performed 48hrs after the first transfection. Following the second round of dsiRNA transfection,
782 SNORD90 OE vectors were transfected 48 hours later. NPCs were then collected 48 hours after
783 the third transfection. DsiRNA sequences and oligos were provided by IDT (supplementary table
784 10). RNA extraction, cDNA synthesis, and RT-qPCR were as described above. One-way
785 ANOVA was used as described above

786

787 **Electrophysiological Recording**

788 *Brain slices preparation*

789 Mice were stereotactically injected with SNORD90-OE or SNORD90-Scramble viral vector as
790 described above.

791
792 3 weeks after the injection, mice received an overdose injection of pentobarbital (100 mg/kg i.p.)
793 and were perfused with carbogenated (95% O₂, 5% CO₂) ice-cold slicing solution containing (in
794 mM): 2.5 KCl, 11 glucose, 234 sucrose, 26 NaHCO₃, 1.25 NaH₂PO₄, 10 MgSO₄, 2 CaCl₂; pH
795 7.4, 340 mOsm. After decapitation, 300 µm coronal slices containing the ACC were prepared in
796 carbogenated ice-cold slicing solution using a vibratome (Leica VT 1200S) and allowed to
797 recover for 20 min at 33°C in carbogenated high osmolarity artificial cerebrospinal fluid (high-
798 Osm aCSF) containing (in mM): 3.2 KCl, 11.8 glucose, 132 NaCl, 27.9 NaHCO₃, 1.34
799 NaH₂PO₄, 1.07 MgCl₂, 2.14 CaCl₂; pH 7.4, 320 mOsm) followed by 40 min incubation at 33°C
800 in carbogenated aCSF containing (in mM): 3 KCl, 11 glucose, 123 NaCl, 26 NaHCO₃, 1.25
801 NaH₂PO₄, 1 MgCl₂, 2 CaCl₂; pH 7.4, 300 mOsm. Subsequently, slices were kept at room
802 temperature (RT) in carbogenated aCSF until use.

803
804 ***Patch-clamp recordings***
805 Slices were then transferred in the recording chamber and superfused (4-5 mL/min) with
806 carbogenated aCSF and recordings performed at RT. Pyramidal neurons of the ACC were
807 visualized with infrared differential interference contrast (DIC) microscopy (BX51W1,
808 Olympus) and an Andor Neo sCMOS camera (Oxford Instruments, Abingdon, UK). Somatic
809 whole-cell voltage-clamp recordings from ACC pyramidal neurons (> 1 GΩ seal resistance, -
810 70 mV holding potential) were performed using a Multiclamp 700B amplifier (Molecular
811 Devices, San Jose, CA, USA). Data were acquired using pClamp 10.7 on a personal computer

812 connected to the amplifier via a Digidata-1440 interface (sampling rate: 20 kHz; low-pass filter:
813 8 kHz). Borosilicate glass pipettes (BF100-58-10, Sutter Instrument, Novato, CA, USA) with
814 resistances 4-6 M Ω were pulled using a laser micropipette puller (P-2000, Sutter Instrument).
815 Data obtained with a series resistance > 20 M Ω or fluctuation more than 20% of the initial values
816 were discarded.

817

818 For sEPSCs recording, pyramidal neurons were clamped at -70 mV in the presence of BIM
819 (20 μ M) with the pipette solution containing (in mM): 125 Cs-methanesulfonate, 8 NaCl, 10
820 HEPES, 0.5 EGTA, 4 Mg-ATP, 0.3 Na-GTP, 20 Phosphocreatine and 5 QX-314 (pH 7.2 with
821 CsOH, 285-290 mOsm).

822

823 Analysis was performed using ClampFit 10.7 and Easy Electrophysiology V2.2
824 (<https://www.easyelectrophysiology.com>), and statistical significance assessed with GraphPad
825 Prism 7.

826

827 **ACKNOWLEDGMENTS:** GT holds a Canada Research Chair (Tier 1) and is supported by
828 grants from the Canadian Institute of Health Research (CIHR) (FDN148374, EGM141899,
829 ENP161427), and by the Fonds de recherche du Québec -Santé (FRQS) through the Quebec
830 Network on Suicide, Mood Disorders, and Related Disorders. CAN-BIND is an Integrated
831 Discovery Program carried out in partnership with, and financial support from, the Ontario Brain
832 Institute, an independent nonprofit corporation, funded partially by the Ontario government. The
833 opinions, results, and conclusions are those of the authors and no endorsement by the Ontario
834 Brain Institute is intended or should be inferred. Additional funding is provided by the Canadian

835 Institutes of Health Research (CIHR). All study medications were independently purchased at
836 wholesale market values. AC is the incumbent of the Vera and John Schwartz Family
837 Professorial Chair in Neurobiology at the Weizmann Institute and the head of the Max Planck
838 Society–Weizmann Institute of Science Laboratory for Experimental Neuropsychiatry and
839 Behavioral Neurogenetics. This work is supported by the German Ministry of Science and
840 Education (IMADAPT, FKZ: 01KU1901); the Ruhman Family Laboratory for Research in the
841 Neurobiology of Stress (AC); research support from Bruno and Simone Licht; the Perlman
842 Family Foundation, founded by Louis L. and Anita M. Perlman (AC); the Adelis Foundation
843 (AC); and Sonia T. Marschak (AC). JPL holds postdoctoral fellowships from the European
844 Molecular Biology Organization (EMBO-ALTF 650-2016), Alexander von Humboldt
845 Foundation, and the Canadian Biomarker Integration Network in Depression (CAN-BIND). J.D.
846 is the incumbent of the Achar Research Fellow Chair in Electrophysiology.

847

848 **AUTHOR CONTRIBUTIONS:** RL and GT conceptualized the project with input from AC,
849 JPL AK, and LMF. JPL performed small RNA sequencing from human clinical samples. PB, FF,
850 BNF, RWL, RM, DJM, SVP, CS, RU, JAF, and SHK participated in the design the sample
851 acquisition of the human clinical trials. RL and LMF performed small RNA sequencing on
852 human post-mortem brain samples. CN and NM contributed to the collection of the human-
853 postmortem samples and molecular analysis. ZA provided bioinformatic support for analysis of
854 sequencing data. AK performed mouse behavioral experiments. ECI and CB provided mouse
855 ACC samples. JD performed electrophysiology experiments; YJB performed surgeries with
856 input from AK and JPL. TPW provided input on electrophysiology experiments. PI performed
857 western blots. RL performed cell culture experiments with input from JY. RL and HH performed

858 m6A experiments. RL and GT wrote the manuscript with input from AK, JPL, JD, JBF, TPW,
859 ECI, CB, PB, FF, BNF, RWL, RM, DJM, SVP, CS, RU, CN, NM, JAF, SHK, and AC.

860

861 **COMPETING INTERESTS:** RM has received consulting and speaking honoraria from
862 AbbVie, Allergan, Eisai, Janssen, KYE, Lallemand, Lundbeck, Neomind, Otsuka, and Sunovion,
863 and research grants from CAN-BIND, CIHR, Janssen, Lallemand, Lundbeck, Nubiyota, OBI and
864 OMHF. JAF has received consulting and speaking fees from Takeda and RBH, and research
865 funding from NSERC, CIHR, and OBI.

866

867 **REFERENCES:**

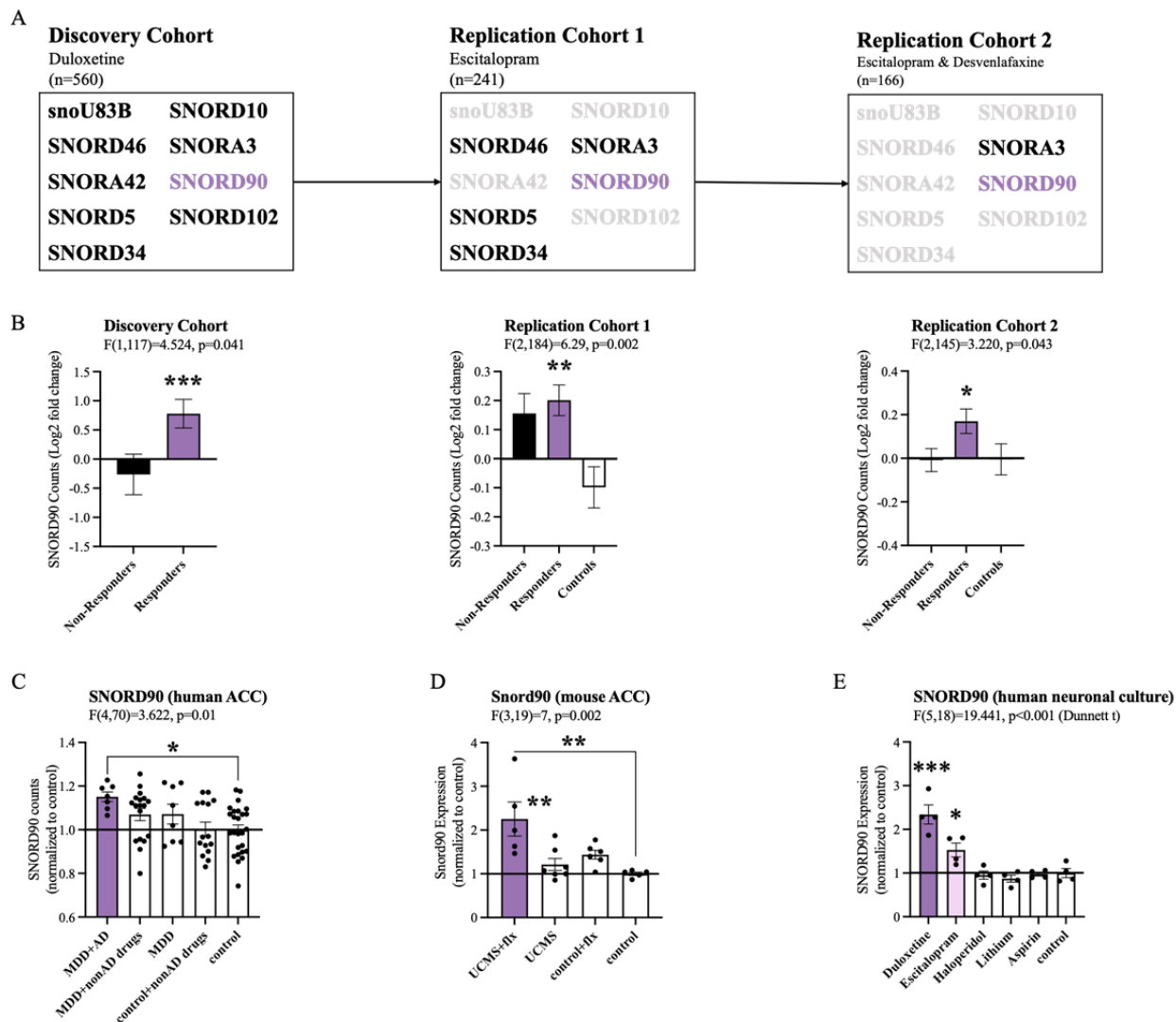
- 868 1. D. J. Brody, Q. Gu, Antidepressant Use Among Adults: United States, 2015-2018. *NCHS*
869 *Data Brief*, 1-8 (2020).
- 870 2. A. Cipriani *et al.*, Comparative efficacy and acceptability of 21 antidepressant drugs for
871 the acute treatment of adults with major depressive disorder: a systematic review and
872 network meta-analysis. *Lancet* **391**, 1357-1366 (2018).
- 873 3. C. J. Harmer, R. S. Duman, P. J. Cowen, How do antidepressants work? New
874 perspectives for refining future treatment approaches. *Lancet Psychiatry* **4**, 409-418
875 (2017).
- 876 4. S. B. Ross, A. L. Renyi, Inhibition of the uptake of tritiated 5-hydroxytryptamine in brain
877 tissue. *Eur J Pharmacol* **7**, 270-277 (1969).
- 878 5. J. Vetulani, F. Sulser, Action of various antidepressant treatments reduces reactivity of
879 noradrenergic cyclic AMP-generating system in limbic forebrain. *Nature* **257**, 495-496
880 (1975).
- 881 6. R. M. Berman *et al.*, Antidepressant effects of ketamine in depressed patients. *Biol*
882 *Psychiatry* **47**, 351-354 (2000).
- 883 7. R. S. Duman, Ketamine and rapid-acting antidepressants: a new era in the battle against
884 depression and suicide. *F1000Res* **7**, (2018).
- 885 8. G. Bonanno *et al.*, Chronic antidepressants reduce depolarization-evoked glutamate
886 release and protein interactions favoring formation of SNARE complex in hippocampus.
887 *J Neurosci* **25**, 3270-3279 (2005).
- 888 9. L. Musazzi, G. Treccani, A. Mallei, M. Popoli, The action of antidepressants on the
889 glutamate system: regulation of glutamate release and glutamate receptors. *Biol*
890 *Psychiatry* **73**, 1180-1188 (2013).
- 891 10. H. S. Mayberg *et al.*, Deep brain stimulation for treatment-resistant depression. *Neuron*
892 **45**, 651-660 (2005).

- 893 11. M. Roet *et al.*, Deep Brain Stimulation for Treatment-Resistant Depression: Towards a
894 More Personalized Treatment Approach. *J Clin Med* **9**, (2020).
- 895 12. M. Herve *et al.*, Translational Identification of Transcriptional Signatures of Major
896 Depression and Antidepressant Response. *Front Mol Neurosci* **10**, 248 (2017).
- 897 13. L. Lestrade, M. J. Weber, snoRNA-LBME-db, a comprehensive database of human
898 H/ACA and C/D box snoRNAs. *Nucleic Acids Res* **34**, D158-162 (2006).
- 899 14. C. Ender *et al.*, A human snoRNA with microRNA-like functions. *Mol Cell* **32**, 519-528
900 (2008).
- 901 15. S. Kishore, S. Stamm, The snoRNA HBII-52 regulates alternative splicing of the
902 serotonin receptor 2C. *Science* **311**, 230-232 (2006).
- 903 16. E. Sharma, T. Sterne-Weiler, D. O'Hanlon, B. J. Blencowe, Global Mapping of Human
904 RNA-RNA Interactions. *Mol Cell* **62**, 618-626 (2016).
- 905 17. S. Kehr, S. Bartschat, P. F. Stadler, H. Tafer, PLEXY: efficient target prediction for box
906 C/D snoRNAs. *Bioinformatics* **27**, 279-280 (2011).
- 907 18. C. Paterson *et al.*, Temporal, Diagnostic, and Tissue-Specific Regulation of NRG3
908 Isoform Expression in Human Brain Development and Affective Disorders. *Am J*
909 *Psychiatry* **174**, 256-265 (2017).
- 910 19. Y. N. Wang *et al.*, Controlling of glutamate release by neuregulin3 via inhibiting the
911 assembly of the SNARE complex. *Proc Natl Acad Sci U S A* **115**, 2508-2513 (2018).
- 912 20. D. Zhang *et al.*, Neuregulin-3 (NRG3): a novel neural tissue-enriched protein that binds
913 and activates ErbB4. *Proc Natl Acad Sci U S A* **94**, 9562-9567 (1997).
- 914 21. M. Falaleeva *et al.*, Dual function of C/D box small nucleolar RNAs in rRNA
915 modification and alternative pre-mRNA splicing. *Proc Natl Acad Sci U S A* **113**, E1625-
916 1634 (2016).
- 917 22. L. P. Benoit Bouvrette, S. Bovaird, M. Blanchette, E. Lecuyer, oRNAmant: a database of
918 putative RNA binding protein target sites in the transcriptomes of model species. *Nucleic*
919 *Acids Res* **48**, D166-D173 (2020).
- 920 23. E. L. Van Nostrand *et al.*, A large-scale binding and functional map of human RNA-
921 binding proteins. *Nature* **583**, 711-719 (2020).
- 922 24. D. P. Patil *et al.*, m(6)A RNA methylation promotes XIST-mediated transcriptional
923 repression. *Nature* **537**, 369-373 (2016).
- 924 25. D. Tollervey, H. Lehtonen, M. Carmo-Fonseca, E. C. Hurt, The small nucleolar RNP
925 protein NOP1 (fibrillarin) is required for pre-rRNA processing in yeast. *EMBO J* **10**, 573-
926 583 (1991).
- 927 26. D. Tollervey, H. Lehtonen, R. Jansen, H. Kern, E. C. Hurt, Temperature-sensitive
928 mutations demonstrate roles for yeast fibrillarin in pre-rRNA processing, pre-rRNA
929 methylation, and ribosome assembly. *Cell* **72**, 443-457 (1993).
- 930 27. J. Kufel, P. Grzechnik, Small Nucleolar RNAs Tell a Different Tale. *Trends Genet* **35**,
931 104-117 (2019).
- 932 28. S. Ke *et al.*, m(6)A mRNA modifications are deposited in nascent pre-mRNA and are not
933 required for splicing but do specify cytoplasmic turnover. *Genes Dev* **31**, 990-1006
934 (2017).
- 935 29. K. D. Meyer, S. R. Jaffrey, Rethinking m(6)A Readers, Writers, and Erasers. *Annu Rev*
936 *Cell Dev Biol* **33**, 319-342 (2017).
- 937 30. S. Zaccara, S. R. Jaffrey, A Unified Model for the Function of YTHDF Proteins in
938 Regulating m(6)A-Modified mRNA. *Cell* **181**, 1582-1595 e1518 (2020).

- 939 31. S. Zaccara, R. J. Ries, S. R. Jaffrey, Reading, writing and erasing mRNA methylation.
940 *Nat Rev Mol Cell Biol* **20**, 608-624 (2019).
- 941 32. L. A. Farrelly *et al.*, Histone serotonylation is a permissive modification that enhances
942 TFIID binding to H3K4me3. *Nature* **567**, 535-539 (2019).
- 943 33. T. Ideue, K. Hino, S. Kitao, T. Yokoi, T. Hirose, Efficient oligonucleotide-mediated
944 degradation of nuclear noncoding RNAs in mammalian cultured cells. *RNA* **15**, 1578-
945 1587 (2009).
- 946 34. D. R. Newman, J. F. Kuhn, G. M. Shanab, E. S. Maxwell, Box C/D snoRNA-associated
947 proteins: two pairs of evolutionarily ancient proteins and possible links to replication and
948 transcription. *RNA* **6**, 861-879 (2000).
- 949 35. D. G. Dimitrova, L. Teyssset, C. Carre, RNA 2'-O-Methylation (Nm) Modification in
950 Human Diseases. *Genes (Basel)* **10**, (2019).
- 951 36. G. Bartolini *et al.*, Neuregulin 3 Mediates Cortical Plate Invasion and Laminar Allocation
952 of GABAergic Interneurons. *Cell Rep* **18**, 1157-1170 (2017).
- 953 37. J. P. Lopez *et al.*, MicroRNAs 146a/b-5 and 425-3p and 24-3p are markers of
954 antidepressant response and regulate MAPK/Wnt-system genes. *Nat Commun* **8**, 15497
955 (2017).
- 956 38. S. H. Kennedy *et al.*, Symptomatic and Functional Outcomes and Early Prediction of
957 Response to Escitalopram Monotherapy and Sequential Adjunctive Aripiprazole Therapy
958 in Patients With Major Depressive Disorder: A CAN-BIND-1 Report. *J Clin Psychiatry*
959 **80**, (2019).
- 960 39. F. Jollant *et al.*, Neural and molecular correlates of psychological pain during major
961 depression, and its link with suicidal ideas. *Prog Neuropsychopharmacol Biol Psychiatry*
962 **100**, 109909 (2020).
- 963 40. A. Kassambara. (R package version 0.6.0., 2020).
- 964 41. A. Dumais *et al.*, Risk factors for suicide completion in major depression: a case-control
965 study of impulsive and aggressive behaviors in men. *Am J Psychiatry* **162**, 2116-2124
966 (2005).
- 967 42. L. M. Fiori *et al.*, miR-323a regulates ERBB4 and is involved in depression. *Mol*
968 *Psychiatry* **26**, 4191-4204 (2021).
- 969 43. J. Lu *et al.*, Generation of serotonin neurons from human pluripotent stem cells. *Nat*
970 *Biotechnol* **34**, 89-94 (2016).
- 971 44. J. P. Lopez *et al.*, miR-1202 is a primate-specific and brain-enriched microRNA involved
972 in major depression and antidepressant treatment. *Nat Med* **20**, 764-768 (2014).
- 973 45. J. P. Guilloux, M. Seney, N. Edgar, E. Sibille, Integrated behavioral z-scoring increases
974 the sensitivity and reliability of behavioral phenotyping in mice: relevance to
975 emotionality and sex. *J Neurosci Methods* **197**, 21-31 (2011).

976

977



978

979

980 **Figure 1:** SNORD90 expression is associated with antidepressant treatment response.

981 **A** Two-way mixed multivariable ANOVA indicates a significant interaction between clinical

982 response (responders/non-responders; between-factor) and treatment course (T0/T8; within

983 factor). Nine snoRNAs displayed significant effects in the discovery cohort. Five out of the nine

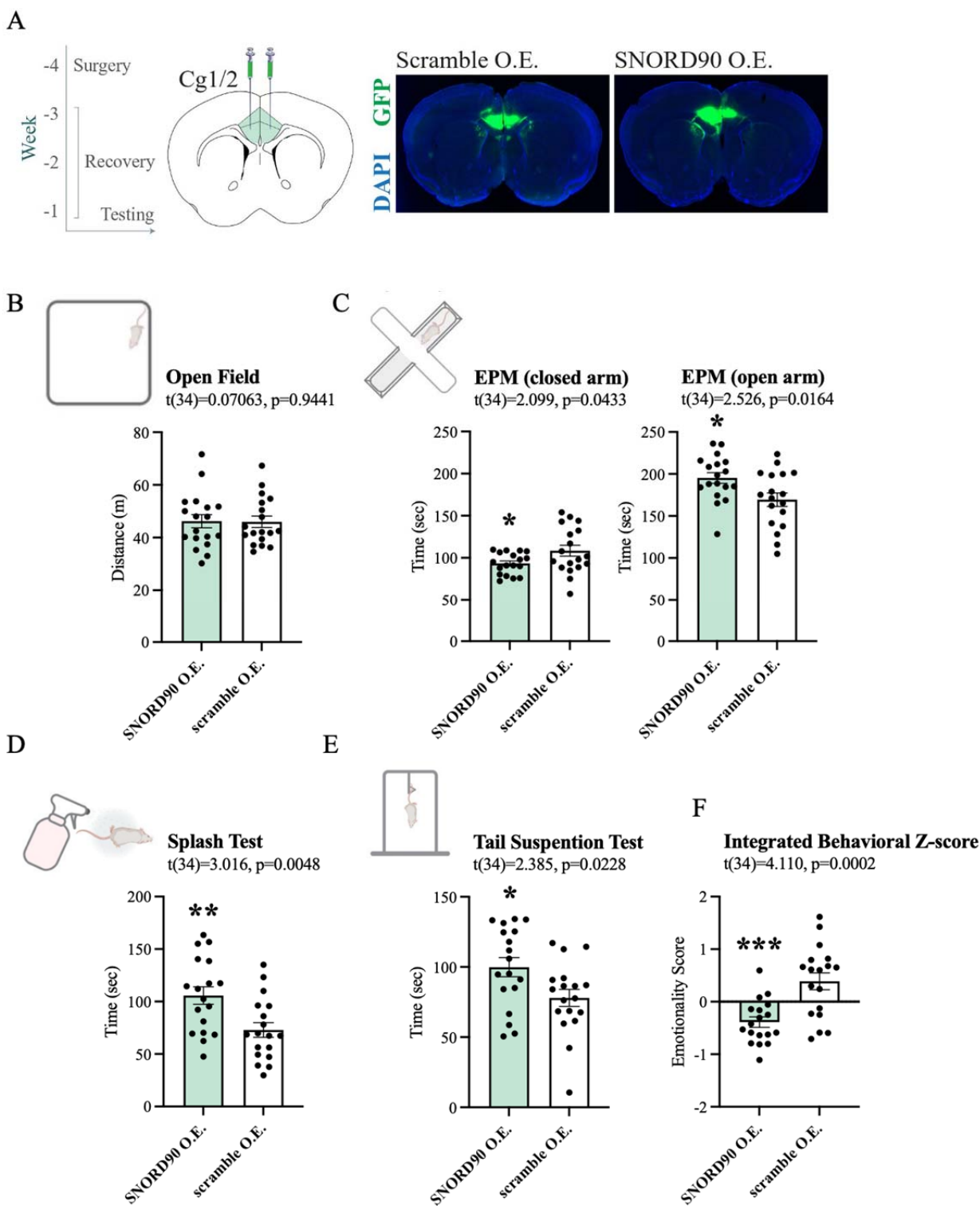
984 snoRNAs were replicated in replication cohort 1 with SNORD90 and SNORA3 further

985 replicated in replication cohort 2. **B** Log₂ fold-change of the expression of SNORD90 before and

986 after antidepressant treatment for all three clinical cohorts. SNORD90 displayed a significantly

987 increased expression after eight weeks of antidepressant treatment specifically in those who
988 responded. **C** Snord90 expression in the ACC of mice that underwent unpredictable chronic mild
989 stress (UCMS) and antidepressant administration. **D** SNORD90 expression in human post-
990 mortem ACC. Samples were separated based on presence or absence of antidepressant drug
991 treatment. **E** SNORD90 expression in human neuronal cultures exposed to various psychotropic
992 drugs. **C-E** Statistical analysis using one-way ANOVA with Bonferroni post-hoc (unless
993 otherwise indicated on the graph). **B-E** All bar plots represent the mean with individual data
994 points as dots. Error bars represent S.E.M. (* $p < 0.05$, ** $p < 0.01$, *** $p < 0.001$).
995

996



997

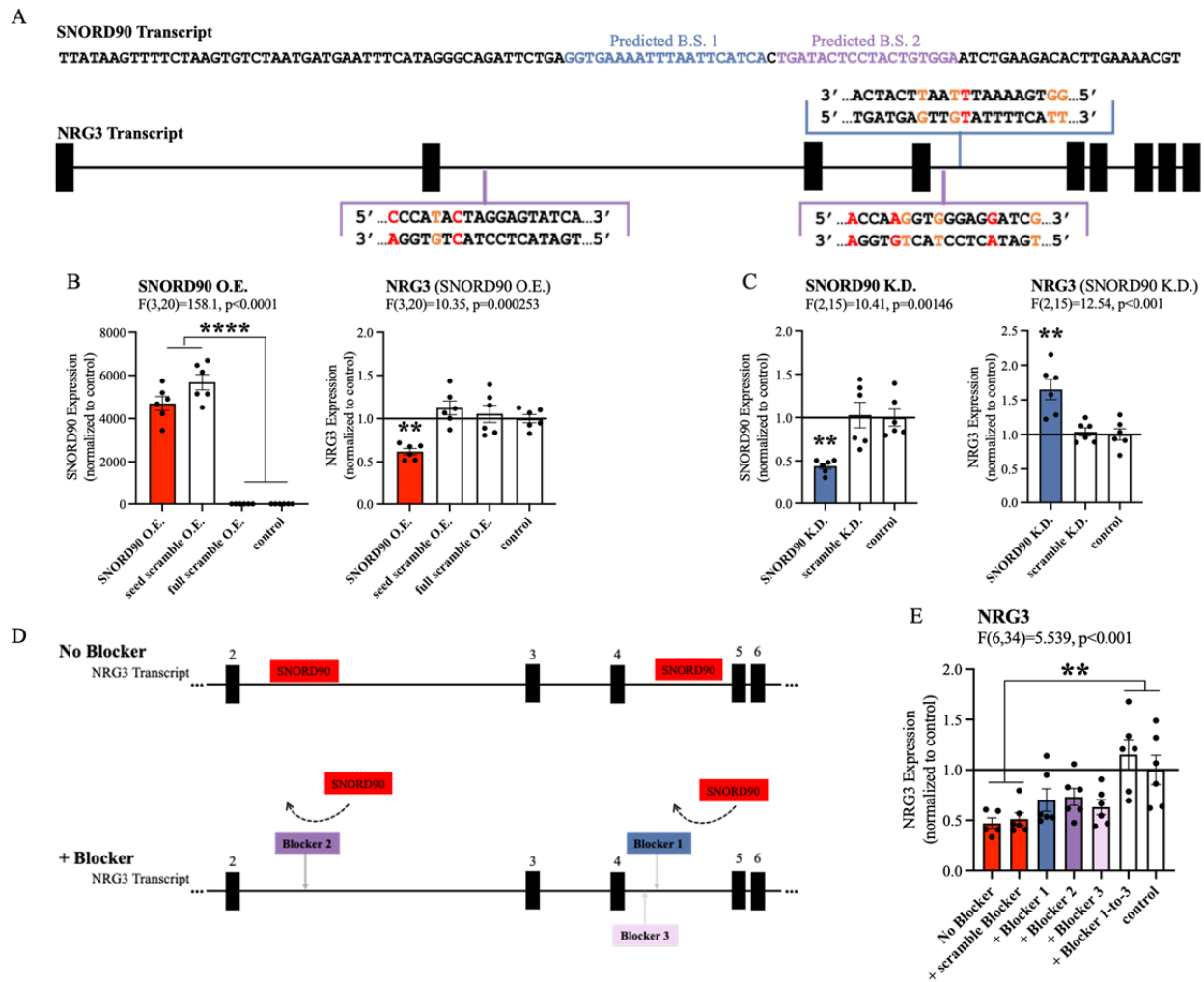
998

999 **Figure 2:** SNORD90 over-expression in mouse Cg1/2 induces anxiolytic and anti depressive-
1000 like behaviors

1001 **A** Timeline of experimental procedure with time (weeks) in relation to behavioral testing.
1002 Surgery for viral injection was performed followed by three weeks of recovery before behavioral
1003 testing (left). Coronal diagram of the mouse brain representing viral injection site (center).
1004 Representative images of GFP expression (green) indicating site specific expression of each
1005 construct (right). **B** The open field test showing total distance traveled in meters. **C** The elevated
1006 plus maze test with total time spent in the closed and open arms of the maze. **D** The splash test
1007 with total grooming time. **E** The tail suspension test with total struggling time. **F** Emotionality z-
1008 score integrating the EPM, SPL, and TST. **C-G** Statistical analysis using student's two-tailed t-
1009 test. All bar plots represent the mean with individual data points as dots. Error bars represent
1010 S.E.M. (* $p < 0.05$, ** $p < 0.01$, *** $p < 0.001$).

1011

1012



1013

1014

1015 **Figure 3: SNORD90 down-regulates NRG3**

1016 **A** Full sequence of mature SNORD90 transcript with highlighted regions, labeled predicted B.S.

1017 1 and predicted B.S. 2, which are predicted to bind to NRG3. Schematic representation of NRG3

1018 pre-mRNA transcript indicating regions on NRG3 where SNORD90 is predicted to bind. The

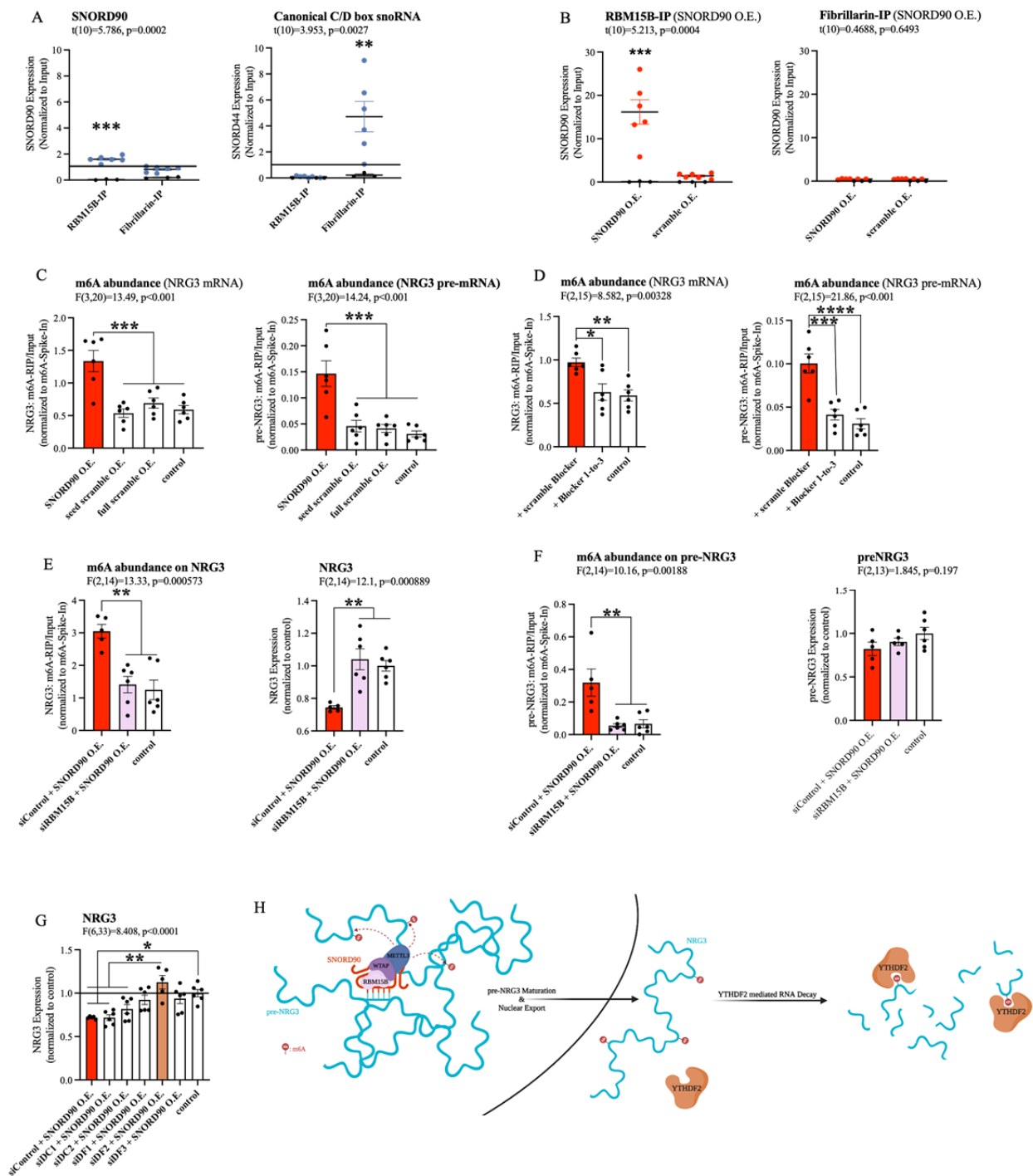
1019 color of the bracket corresponds to predicted B.S.-1 or predicted B.S.-2. **B** Expression of

1020 SNORD90 (left) and NRG3 (right) after over-expressing SNORD90 or scrambled controls

1021 (right). **C** Expression of SNORD90 (left) and NRG3 (right) after knocking-down SNORD90

1022 with antisense oligonucleotides (ASO) and scrambled ASO. **D** Schematic representation of co-
1023 transfection of SNORD90 over-expression vector without target blockers (top) and with target
1024 blockers (bottom). Target blockers were designed to bind to regions SNORD90 is predicted to
1025 bind, consequently blocking SNORD90 from interacting with those regions on NRG3 (bottom).
1026 **E** Expression of NRG3 after over-expression of SNORD90 and target blockers. Target blockers
1027 were included one site at a time and all three sites together. **B-D, F** All bar plots represent the
1028 mean with individual data points as dots. Error bars represent S.E.M. All statistical analysis
1029 utilized a one-way ANOVA with Bonferroni post-hoc (* $p < 0.05$, ** $p < 0.01$, *** $p < 0.001$).
1030

1031



1032

1033

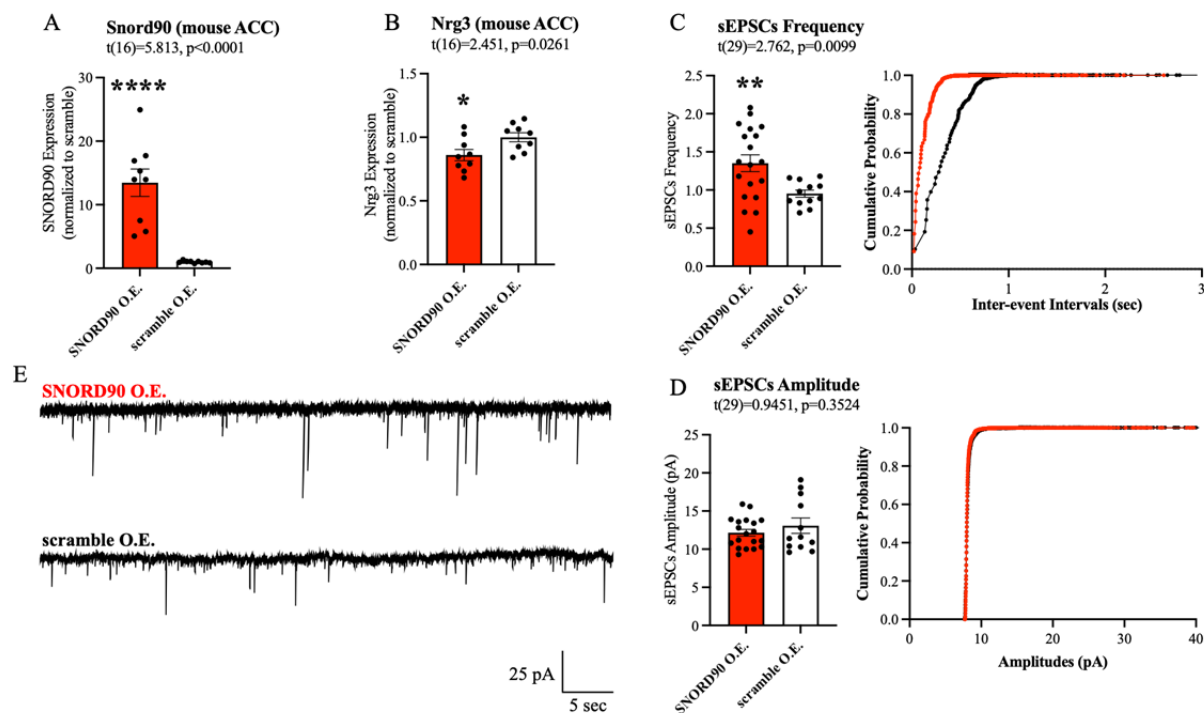
1034

Figure 4: SNORD90 is a guide RNA for RBM15B and increases m6A abundance on NRG3

1035 **A** Abundance of SNORD90 (left) and canonical snoRNA (SNORD44; right) in RBM15B-IP and
1036 fibrillarin-IP fractions. **B** Abundance of SNORD90 in RBM15B-IP (left) and fibrillarin-IP (right)
1037 following over-expression of SNORD90 or scramble control. **C** Abundance of m6A
1038 modifications on NRG3 mRNA (left) and NRG3 pre-mRNA (right) following over-expression of
1039 SNORD90 or scramble controls. **D** Abundance of m6A modifications on NRG3 mRNA (left)
1040 and NRG3 pre-mRNA (right) following SNORD90 overexpression with target blockers. **E**
1041 Abundance of m6A modifications on NRG3 (left) and NRG3 expression (right) following
1042 RBM15B knock-down (siRBM15B) or negative control (siControl) and SNORD90 over-
1043 expression. **F** Same as E but on NRG3 pre-mRNA. **G** Expression of NRG3 after knocking-down
1044 m6A reader proteins followed by over-expression of SNORD90. **H** Schematic overview of
1045 SNORD90 regulation of NRG3 expression. SNORD90 interacts with m6A writer complex in the
1046 nucleus and guides this complex onto NRG3 increasing m6A abundance. The increase in m6A
1047 abundance is not recognized until NRG3 reaches the cytoplasm where it undergoes YTHDF2
1048 mediated RNA decay. All bar plots represent the mean with individual data points as dots. Error
1049 bars represent S.E.M. Statistical analysis utilized as follows: **A-B** Student's two-tailed t test. **E**
1050 Pearson correlation. **C-D, F-H** One-way ANOVA with Bonferroni post-hoc (* $p < 0.05$, ** $p < 0.01$,
1051 *** $p < 0.001$).

1052

1053



1054

1055

1056 **Figure 5:** SNORD90 induced down-regulation of Nrg3 increases glutamatergic

1057 neurotransmission

1058 **A** qPCR confirmation of Snord90 over-expression in *cg1/2*. **B** Nrg3 expression after Snord90

1059 over-expression. **C-E** Whole-cell patch-clamp recordings in *Cg1/2* acute brain slices from mice

1060 over-expressing SNORD90 or scramble control. sEPSCs were recorded from pyramidal neurons

1061 at -70 mV. **A-C & E** Statistical analysis using student's two-tailed T-test. All bar plots represent

1062 the mean with individual data points as dots. Error bars represent S.E.M. (*p<0.05, **p<0.01,

1063 ***p<0.001).

1064

Supplementary Materials for

SNORD90 induces glutamatergic signaling following treatment with monoaminergic antidepressants

Rixing Lin[†], Aron Kos[†], Juan Pablo Lopez, Julien Dine, Pascal Ibrahim, Jennie Yang, Laura M. Fiori, Yair Ben-Efraim, Zahia Aouabed, Haruka Mitsuhashi, Tak Pan Wong, El Cherif Ibrahim, Catherine Belzung, Pierre Blier, Faranak Farzan, Benicio N. Frey, Raymond W. Lam, Roumen Milev, Daniel J. Müller, Sagar V. Parikh, Claudio Soares, Rudolf Uher, Corina Nagy, Naguib Mechawar, Jane A. Foster, Sidney H. Kennedy, Alon Chen*, and Gustavo Turecki*

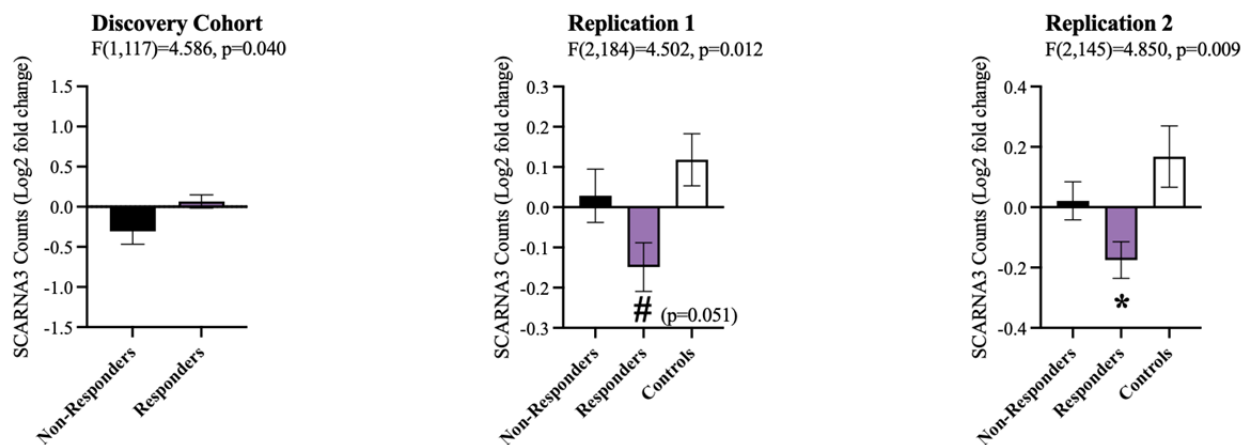
[†]These authors contributed equally to this work
*Corresponding author. Email: gustavo.turecki@mcgill.ca

This PDF file includes:

Figs. S1 to S10

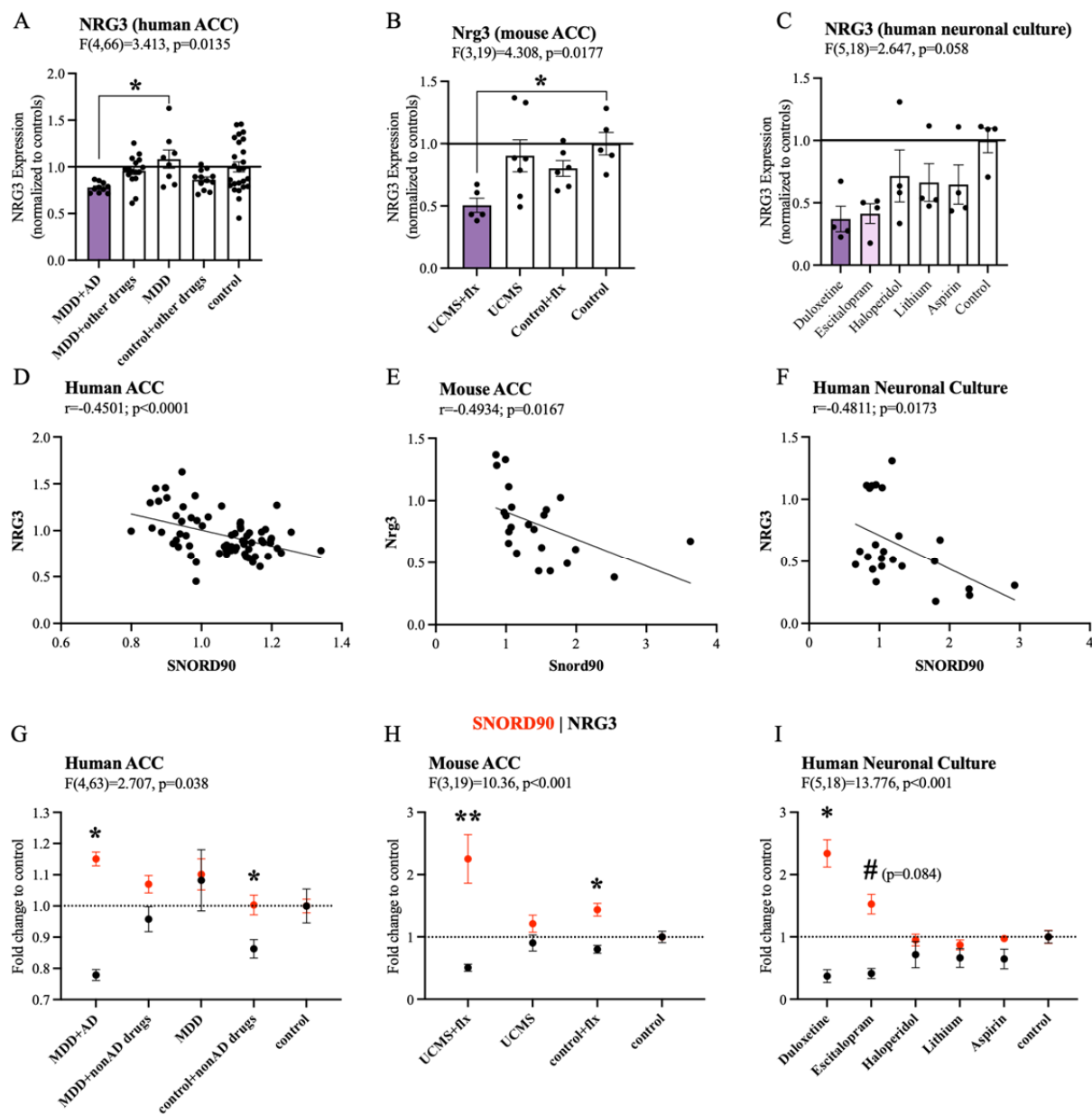
Other Supplementary Material for this manuscript includes the following:

Table S1 to S10 (.xlsx)



Supplementary Figure 1: SCARNA3 expression in human clinical cohorts (related to figure 1)

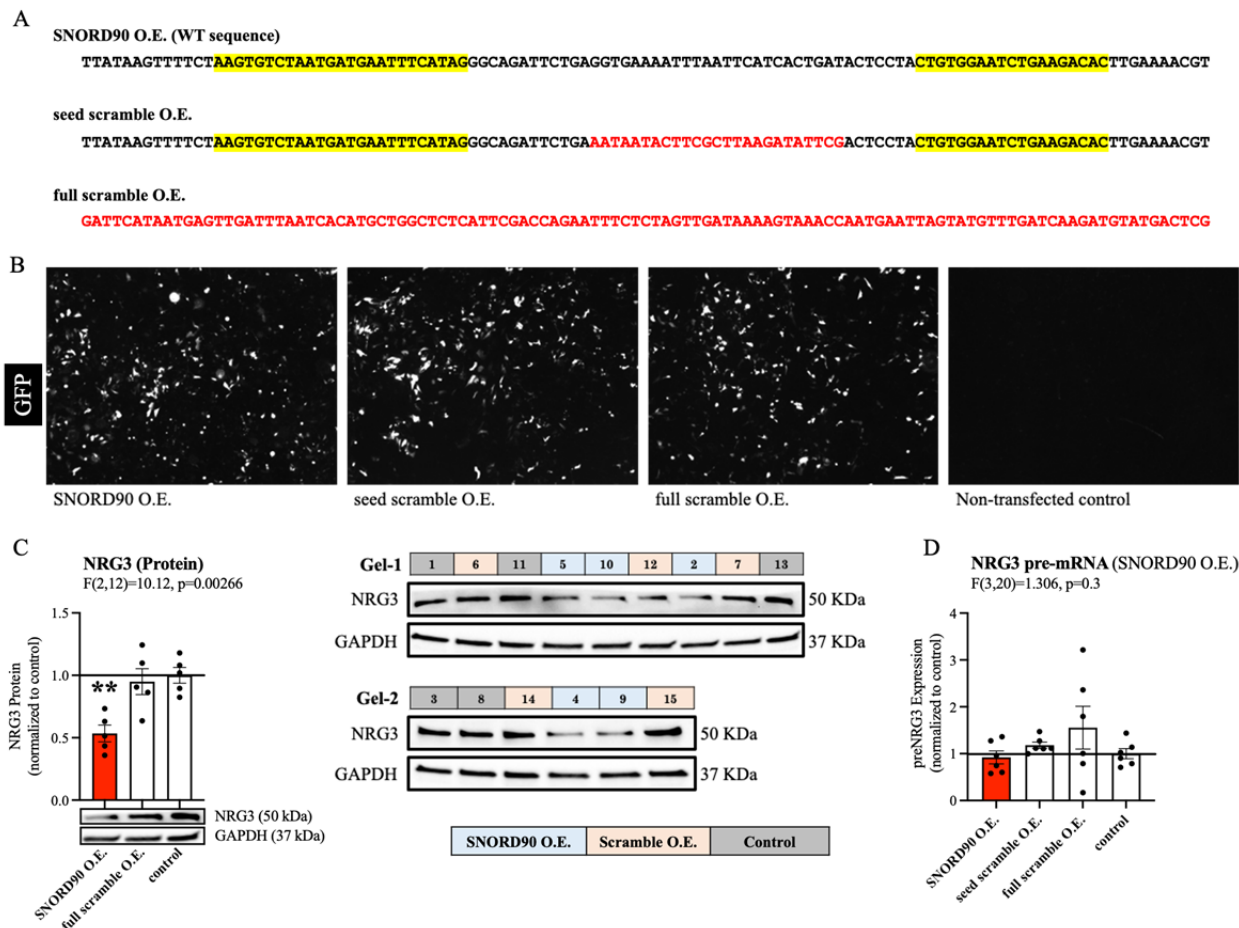
Log2 fold-change of the expression of SCARNA3 before and after antidepressant treatment for all three clinical cohorts. SCARNA3 displayed inconsistent expression after eight weeks of antidepressant treatment.



Supplementary Figure 2: NRG3 expression negatively correlates with SNORD90 in the context of antidepressant (related to figure 1)

A Nrg3 expression in the ACC of mice that underwent unpredictable chronic mild stress (UCMS) and antidepressant administration. **B** NRG3 expression in human post-mortem ACC.

Samples were separated based on presence or absence of antidepressant drug treatment. **C** NRG3 expression in human neuronal cultures exposed to various psychotropic drugs. **D-F** Correlation between SNORD90 and NRG3 expression in each of the respective experiments listed in A-C. **G-I** SNORD90 (red) and NRG3 (black) fold change in relation to control conditions. SNORD90 and NRG3 displayed the most opposing direction of expression in groups exposed to antidepressants. **A-C** Statistical analysis using one-way ANOVA with Bonferroni post-hoc. **D-F** Pearson correlation. **G-I** Statistical analysis using two-way mixed ANOVA with Bonferroni post-hoc. All bar plots represent the mean with individual data points as dots. Error bars represent S.E.M. (* $p < 0.05$, ** $p < 0.01$).



Supplementary Figure 3: SNORD90 over-expression in human NPCs (related to figure 3)

A Sequences of each over-expressed transcript. Red indicates scrambled sequence and black indicates wild-type sequence. Yellow highlight indicates where forward and reverse primers bind for qPCR quantification. Over-expression of SNORD90 WT transcript and seed scramble will be detected by our primers however full scramble will not. **B** Image of NPC 48hrs post-transfection. White is the expression of GFP to confirm successful transfection. **C** Quantification of NRG3 protein levels following SNORD90 over-expression. NRG3 protein levels were significantly reduced after SNORD90 over-expression (left). Western blots where samples were equally

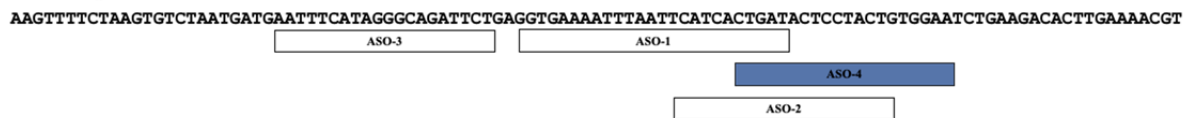
distributed between two separate gels and randomly assigned a well (right). **D** Expression of NRG3 pre-mRNA following SNORD90 over-expression. **C-D** Statistical analysis using one-way ANOVA with Bonferroni post-hoc. All bar plots represent the mean with individual data points as dots. Error bars represent S.E.M. (* $p < 0.05$, ** $p < 0.01$).

Supplementary Figure 3C-source data

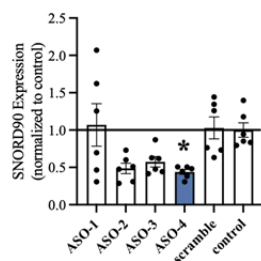
Source data for western blots for supplementary figure 3C including original unedited files of each western blot.

A

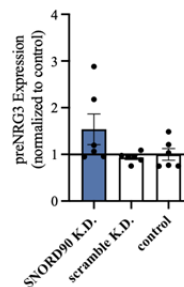
SNORD90 Transcript



B SNORD90 ASO K.D. Screen
F(5,30)=4.294, p=0.005 (Dunnett t)

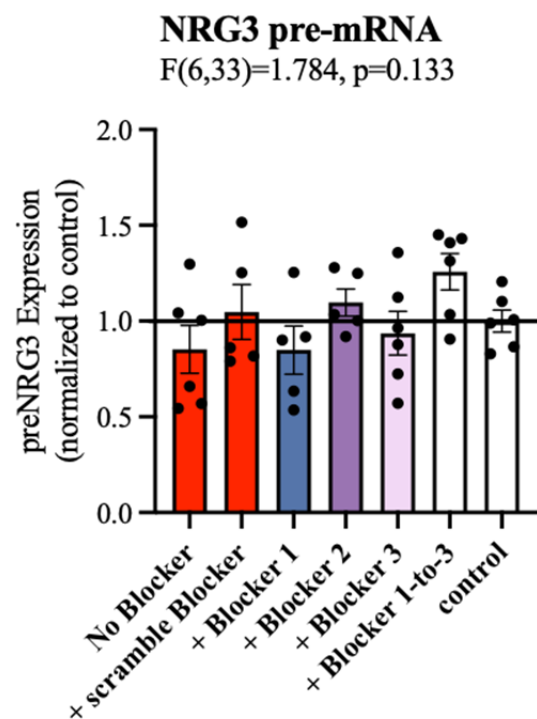


C NRG3 pre-mRNA (SNORD90 O.E.)
F(2,15)=2.627, p=0.105



Supplementary Figure 4: SNORD90 knock-down in human NPCs (related to figure 3)

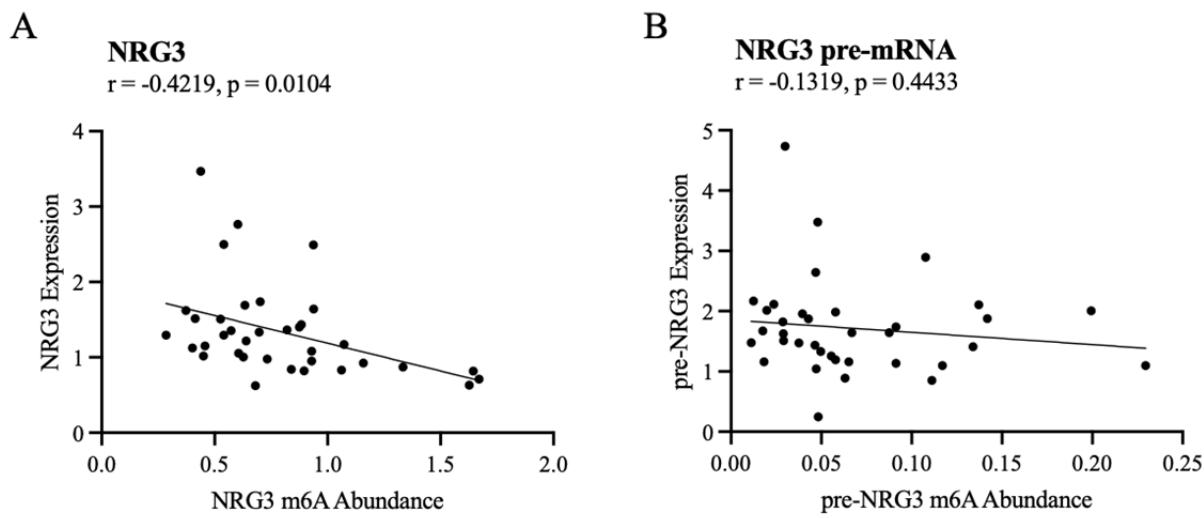
A Schematic diagram indicating where each ASO is designed to bind onto SNORD90. **B** Screen of all four ASOs to determine which ASO produced the best knock-down of SNORD90. **C** Expression of NRG3 pre-mRNA after SNORD90 knock-down. **B-C** Statistical analysis using one-way ANOVA with Bonferroni post-hoc (unless otherwise indicated on the graph). All bar plots represent the mean with individual data points as dots. Error bars represent S.E.M. (*p<0.05).



Supplementary Figure 5: SNORD90 over-expression and NRG3 target blockers (related to figure 3)

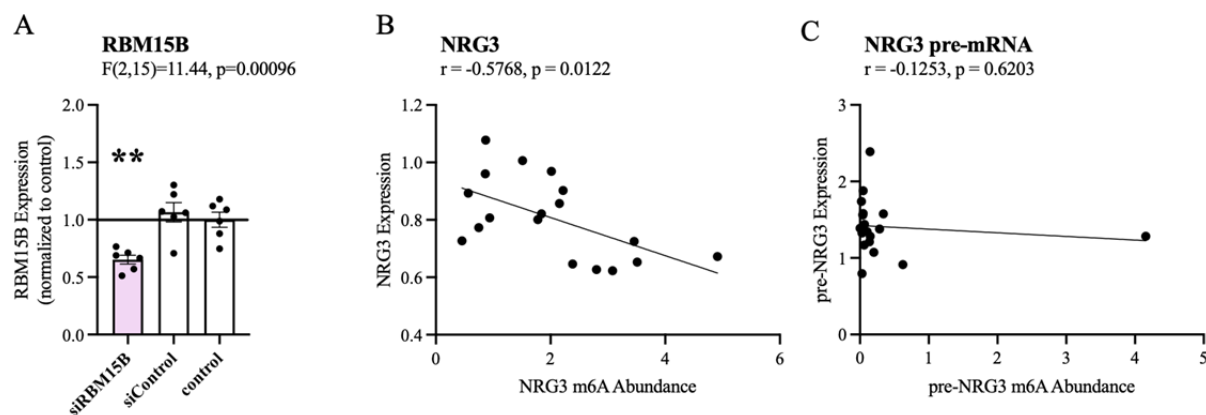
Expression of NRG3 pre-mRNA after SNORD90 over-expression followed by NRG3 target blockers. Statistical analysis using one-way ANOVA with Bonferroni post-hoc (unless otherwise indicated on the graph). All bar plots represent the mean with individual data points as dots.

Error bars represent S.E.M.



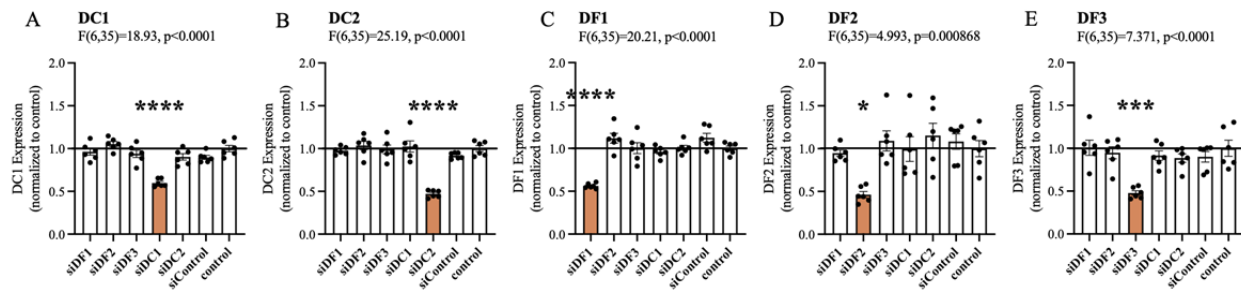
Supplementary Figure 6: m6A abundance on NRG3 is related to expression (related to figure 4)

A Correlation of total m6A abundance on NRG3 and NRG3 expression. **B** Correlation of total m6A abundance on NRG3 pre-mRNA and NRG3 pre-mRNA expression. **A-B** person correlation



Supplementary Figure 7: RBM15B knock-down (related to figure 4)

A qPCR validation of RBM15B knock-down using dsRNAs. **B-C** Correlation of total m6A abundance on NRG3 or NRG3 pre-mRNA and expression. **B-C** Person correlation. **A** Statistical analysis using one-way ANOVA with Bonferroni post-hoc. All bar plots represent the mean with individual data points as dots. Error bars represent S.E.M. (** $p < 0.01$).



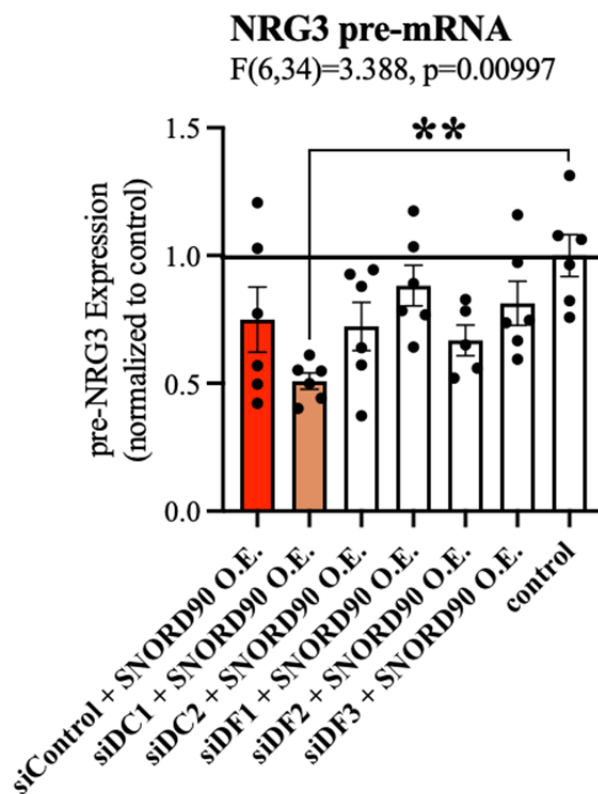
Supplementary Figure 8: m6A-reader knock-down (related to figure 4)

A-E qPCR validation of each respective m6A-reader knock-down using dsiRNAs. **A-E**

Statistical analysis using one-way ANOVA with Bonferroni post-hoc. All bar plots represent the

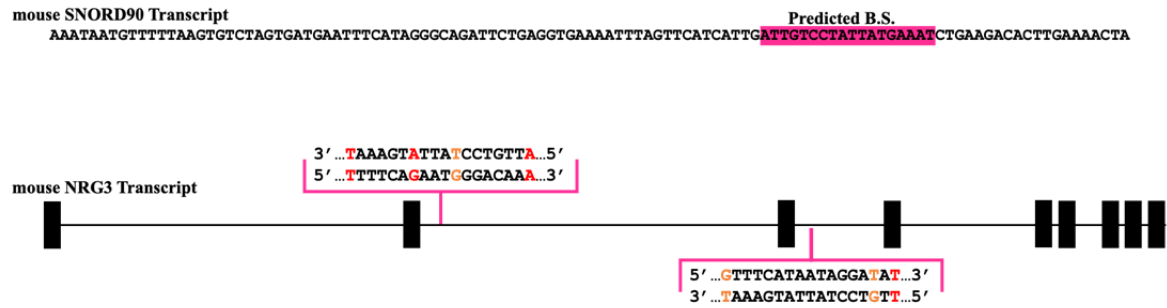
mean with individual data points as dots. Error bars represent S.E.M. (* p<0.05, **p<0.01,

p<0.001, *p<0.0001).



Supplementary Figure 9: Expression of NRG3 pre-mRNA after m6A-reader knock-down (related to figure 4)

Expression of NRG3 pre-mRNA following m6A-reader knock-down and SNORD90 over-expression. Statistical analysis using one-way ANOVA with Bonferroni post-hoc. All bar plots represent the mean with individual data points as dots. Error bars represent S.E.M. (**p<0.01).



Supplementary Figure 10: Snord90-nrg3 interaction is conserved in mice (related to figure 5)

Schematic diagram showing predicted interaction sites between Snord90 and Nrg3 in mice

Supplementary Table 1 to 10

Supp. Table 1 (separate file). Summary statistics for small RNA sequencing analysis in human clinical discovery cohort

Supp. Table 2 (separate file). Summary statistics for small RNA sequencing analysis in human clinical replication 1 cohort

Supp. Table 3 (separate file). Summary statistics for small RNA sequencing analysis in human clinical replication 2 cohort

Supp. Table 4 (separate file). SNORD90 BLAST alignment results

Supp. Table 5 (separate file). SNORD90 PLEXY target prediction results (human)

Supp. Table 6 (separate file). SNORD90 RNA binding protein motif prediction results

Supp. Table 7 (separate file). SNORD90 PLEXY target prediction results (mouse)

Supp. Table 8 (separate file). qPCR primer sequences

Supp. Table 9 (separate file). ASO sequences

Supp. Table 10 (separate file). dsRNA sequences